

*Supporting Information for*

**Anion- $\pi$  and Anion- $\pi$ -Radical Interactions in Bis(triphenylphosphonium)-  
Naphthalene Diimide Salts**

Chee Koon Ng,<sup>a</sup> Teck Lip Dexter Tam,<sup>a\*</sup> Fengxia Wei,<sup>a</sup> Xuefeng Lu,<sup>b</sup> Jishan Wu<sup>b</sup>

<sup>a</sup> *Institute of Materials Research and Engineering (IMRE), Agency of Science, Technology and Research (A\*STAR), 2 Fusionopolis Way, Innovis, #08-03, Singapore 138634, Singapore.*

<sup>b</sup> *Department of Chemistry, National University of Singapore, 3 Science Drive 3, Singapore, 117543, Singapore.*

**Table of Contents**

1. Experimental section.....	S2
1.1 General .....	S2
1.1.1 Photoinduced electron transfer .....	S3
1.2 Synthetic procedures and characterization data.....	S4
2. X-ray crystallographic structures, selected crystal data, data collection, and refinement parameters .....	S9
3. Characterization data of DTPP-NDI salts .....	S19
4. <sup>1</sup> H, <sup>13</sup> C{ <sup>1</sup> H} NMR, MALDI-TOF and ESI mass spectra of synthesized compounds.....	S26
5. References.....	S56

## 1. Experimental section

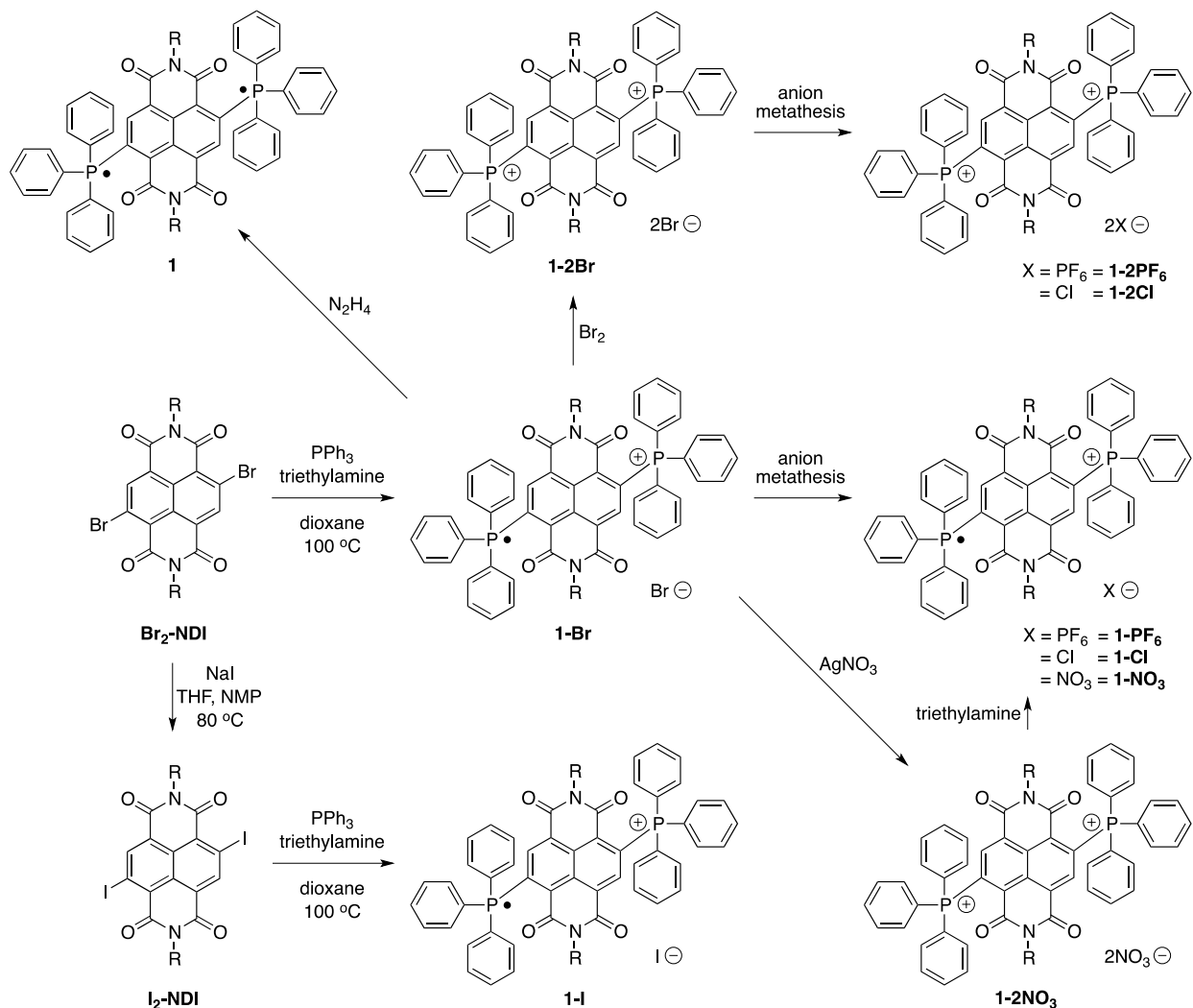
### 1.1. General

All reagents were purchased from Sigma Aldrich other than 2,6-dibromo-*N,N'*-bis(2-ethylhexyl)-1,8:4,5-naphthalene tetracarboxdiimide (TCI).  $^1\text{H}$  and  $^{13}\text{C}\{^1\text{H}\}$  NMR were performed on JEOL 500MHz NMR system with chemical shifts referenced to the deuterated solvent. The  $^{19}\text{F}$ ,  $^{35}\text{Cl}$ ,  $^{81}\text{Br}$  and  $^{127}\text{I}$  NMR spectra were recorded on a JEOL 500MHz NMR operating at 470.39, 49.94, 134.89 and 99.94 MHz for  $^{19}\text{F}$ ,  $^{35}\text{Cl}$ ,  $^{81}\text{Br}$  and  $^{127}\text{I}$  respectively. The  $^{19}\text{F}$ ,  $^{35}\text{Cl}$ ,  $^{81}\text{Br}$  and  $^{127}\text{I}$  NMR spectra were externally referenced to 1.0 M aqueous ( $\text{D}_2\text{O}$ ) solutions of KF, NaCl, NaBr and NaI respectively, at -125.30 ppm ( $^{19}\text{F}$ ) and 0 ppm ( $^{35}\text{Cl}$ ,  $^{81}\text{Br}$  and  $^{127}\text{I}$ ). UV-Vis-NIR absorption spectra were recorded on a Shimadzu UV-3101PC UV-VIS-NIR Spectrophotometer. Cyclic voltammetry (CV) experiments were performed using Autolab potentiostat (model PGSTAT30) by Echochimie. All CV measurements were recorded in dry acetonitrile with 0.1 M tetra-*n*-butylammonium hexafluorophosphate as supporting electrolyte (scan rate of  $100\text{ mV}\cdot\text{s}^{-1}$ ), glassy carbon disk as working electrode, gold disk as counter electrode and Ag/AgCl as reference electrode. Ferrocene was used as external standard (HOMO = oxidation onset =  $-4.80\text{ eV}$ ). LUMO values of the compounds were calculated using the formula:  $-4.80 - (\text{reduction onset of compound})$ . Continuous wave X-band ESR spectra were obtained with a JEOL (FA200) spectrometer at room temperature using dry dichloromethane as solvent and DPPH as standard. XPS spectra were measured on powder samples using VG Thermo Escalab 220i -XL X-ray photoelectron spectroscopy system. XPS data is analyzed using Thermo Advantage v4.12. Single crystals were submitted to X-ray Diffraction Laboratory in National University of Singapore for single crystal structure. A solvent mask was applied during refinement to model the disordered solvent molecules in the structure for 1-Cl. ESI-MS measurements were performed on Shimadzu LCMS-IT-TOF, isotope distribution patterns were used as a composition proof in addition to  $m/z$  signal. Elemental analysis data were not included as the compounds contained phosphorous atoms and could not be fully combusted as phosphorous can lead to the formation of refractory complexes with carbon.<sup>1</sup>

### **1.1.1 Photoinduced electron transfer**

Photoinduced electron transfer experiments were performed using a white LED light of 10 lumens. **1-NO<sub>3</sub>** was dissolved in either acetonitrile or chloroform in a cuvette and the UV-vis spectrum of the pristine solution was acquired. The LED light was then shone on the cuvette for one minute and the UV-vis spectrum was subsequently acquired. This process was repeated for a total of ten readings in acetonitrile and chloroform each.

## 1.2. Synthetic procedures and characterization data



**Scheme S1.** Syntheses of the BTPP-NDI compounds.

**I<sub>2</sub>-NDI.** 1 g of 2,6-dibromo-*N,N'*-bis(2-ethylhexyl)-1,8:4,5-naphthalene tetracarboxdiimide (**Br<sub>2</sub>-NDI**, 1.54 mmol), 9.24 g of sodium iodide (61.60 mmol), 50 mL of *n*-methyl-2-pyrrolidone and 50 mL of THF was added into a two-necked round-bottom flask with a condenser attached. The reaction setup was purged with nitrogen and heated at 80°C for 24 hours. The reaction mixture was cooled in an ice bath, filtered and washed with ethanol. The solids were re-dissolved in 50 mL of *n*-methyl-2-pyrrolidone and 50 mL of tetrahydrofuran and 9.24 g of sodium iodide (61.60 mmol) was added, purged with nitrogen and heated at 80°C for 24 hours again. The reaction mixture was cooled in an ice bath, filtered and washed with ethanol. The solid was recrystallized

from hot tetrahydrofuran. Yield: 880 mg (77%). Yellow orange solids.  $^1\text{H}$  NMR (500 MHz,  $\text{DMSO-}d_6$ )  $\delta$  9.33 (s, 2H), 4.20 – 4.12 (m, 4H), 1.97 – 1.92 (m, 2H), 1.38 – 1.29 (m, 16H), 0.93 (t,  $J = 7.4$  Hz, 6H), 0.88 (t,  $J = 7.1$  Hz, 6H).

**1-Br.** The synthesis was modified from a previously reported procedure using 1,4-dioxane instead of benzonitrile.<sup>2</sup> 500 mg of 2,6-dibromo-*N,N'*-bis(2-ethylhexyl)-1,8:4,5-naphthalene tetracarboxdiimide ( $\text{Br}_2\text{-NDI}$ , 0.77 mmol), 161.4  $\mu\text{L}$  of triethylamine (TEA, 1.16 mmol), 809 mg of  $\text{PPh}_3$  (3.08 mmol) and 40 mL of dry 1,4-dioxane was added into a Schlenk flask under  $\text{N}_2$  and sealed with a rubber septum. The reaction setup then heated at  $100^\circ\text{C}$  for 2 hours and then cooled to room temperature. The solvent was removed under vacuum and the crude residue was purified by column chromatography (dichloromethane, then dichloromethane/methanol 9:1). The compound was subsequently dissolved in some dichloromethane and triturated with diethyl ether. Yield: 675 mg (80%). Dark-green solid. Single crystals were obtained by layering diethyl ether on a concentrated solution of 1-Br in acetonitrile.  $^{81}\text{Br}$  NMR (134.89 MHz,  $\text{CD}_3\text{CN}$ )  $\delta$  86.32. ESI-MS  $m/z$ : 1012.44  $[\text{M-Br}]^+$ ; calcd. for  $\text{C}_{66}\text{H}_{66}\text{N}_2\text{O}_4\text{P}_2$   $[\text{M-Br}]^+$ : 1012.45. HRMS-ESI-MS  $m/z$ : 1012.4523  $[\text{M-Br}]^+$ ; calcd. for  $\text{C}_{66}\text{H}_{66}\text{N}_2\text{O}_4\text{P}_2$   $[\text{M-Br}]^+$ : 1012.4492.

**1-I.** This compound was prepared in a similar manner as 1-Br using 500 mg of 2,6-diiodo-*N,N'*-bis(2-ethylhexyl)-1,8:4,5-naphthalene tetracarboxdiimide ( $\text{I}_2\text{-NDI}$ , 0.67 mmol), 140.9  $\mu\text{L}$  of triethylamine (TEA, 1.01 mmol), 707 mg of  $\text{PPh}_3$  (2.70 mmol) and 40 mL of dry 1,4-dioxane. Yield: 530 mg (69%). Dark-green solid. Single crystals were obtained by layering diethyl ether on a concentrated solution of 1-I in acetonitrile. ESI-MS  $m/z$ : 1012.44  $[\text{M-I}]^+$ ; calcd. for  $\text{C}_{66}\text{H}_{66}\text{N}_2\text{O}_4\text{P}_2$   $[\text{M-I}]^+$ : 1012.45. HRMS-ESI-MS  $m/z$ : 1012.4527  $[\text{M-I}]^+$ ; calcd. for  $\text{C}_{66}\text{H}_{66}\text{N}_2\text{O}_4\text{P}_2$   $[\text{M-I}]^+$ : 1012.4492.

**1-PF<sub>6</sub>.** 50 mg of 1-Br (0.046 mmol) was dissolved in 8 mL of MeOH in a round-bottom flask. 150 mg of  $\text{NH}_4\text{PF}_6$  (0.91 mol) was dissolved in 5 mL MeCN and added to the reaction mixture. The reaction mixture was allowed to stir overnight at room temperature and precipitated into 50 mL of DI water. The precipitate was filtered, washed with DI water and dried under vacuum. Yield: 45 mg (85%). Dark-green solid. Single crystals were obtained by layering diethyl ether on a concentrated solution of 1-PF<sub>6</sub> in acetonitrile.  $^{19}\text{F}$  NMR (470.39 MHz,  $\text{CD}_3\text{CN}$ )  $\delta$  -74.78, -76.28.

$^{19}\text{F}$  NMR (470.39 MHz,  $\text{CDCl}_3$ )  $\delta$  -76.04, -77.57. ESI-MS  $m/z$ : 1012.44  $[\text{M-PF}_6]^+$ ; calcd. for  $\text{C}_{66}\text{H}_{66}\text{N}_2\text{O}_4\text{P}_2$   $[\text{M-PF}_6]^+$ : 1012.45.

**1-Cl.** 200 mg of 1-Br (0.183 mmol) was dissolved in 5 mL of chloroform. 262 mg of silver chloride (1.830 mmol) and 5 mL of methanol were added and the suspension was sonicated in the dark for 30 mins. The suspension was allowed to stir overnight under light illumination. The reaction was filtered through 0.45  $\mu\text{m}$  PTFE filter and solvent was removed using rotary evaporation. The solids were purified using column chromatography (dichloromethane/methanol 9:1). Dark-green solid. Single crystals were obtained by layering diethyl ether on a concentrated solution of 1-Cl in acetonitrile.  $^{35}\text{Cl}$  NMR (49.94 MHz,  $\text{CD}_3\text{CN}$ )  $\delta$  37.89.  $^{35}\text{Cl}$  NMR (49.94 MHz,  $\text{CDCl}_3$ )  $\delta$  -2.26. ESI-MS  $m/z$ : 1012.45  $[\text{M-Cl}]^+$ ; calcd. for  $\text{C}_{66}\text{H}_{66}\text{N}_2\text{O}_4\text{P}_2$   $[\text{M-Cl}]^+$ : 1012.45.

**1-2Br.** 40 mg of 1-Br (0.037 mmol) was dissolved in 5 mL of chloroform. 4  $\mu\text{L}$  of  $\text{Br}_2$  (0.078 mmol) was added and the dark green solution turned brown. The solution was allowed to stir for one hour at room temperature and the solvent was removed under vacuum. The compound was dissolved in some dichloromethane and triturated with diethyl ether. The precipitate was filtered, washed with diethyl ether and dried under vacuum. Yield: 40 mg (92%). Orange solid. Single crystals were obtained by layering diethyl ether on a concentrated solution of 1- $\text{PF}_6$  in chloroform.  $^1\text{H}$  NMR (500 MHz,  $\text{CDCl}_3$ )  $\delta$  8.48 (dd,  $J$  = 14.1, 1.2 Hz, 2H), 7.88 – 7.63 (m, 30H), 3.73 – 3.58 (m, 4H), 1.29 (br s, 2H), 1.17 – 0.80 (m, 16H), 0.78 (t,  $J$  = 7.1 Hz, 6H), 0.55 (t,  $J$  = 7.3 Hz, 6H).  $^{13}\text{C}\{^1\text{H}\}$  NMR (125 MHz,  $\text{CDCl}_3$ )  $\delta$  162.38, 161.06, 137.32, 137.22, 134.55, 134.18, 134.11, 132.41, 132.11, 132.04, 130.46, 130.35, 129.25, 129.15, 125.93, 125.21, 120.71, 119.95, 45.55, 37.42, 30.38, 28.56, 23.49, 23.07, 14.31, 10.46.  $^{31}\text{P}$  NMR (202 MHz,  $\text{CDCl}_3$ )  $\delta$  31.33.

ESI-MS  $m/z$ : 1012.45  $[\text{M-2Br}]^+$ ; calcd. for  $\text{C}_{66}\text{H}_{66}\text{N}_2\text{O}_4\text{P}_2$   $[\text{M-2Br}]^+$ : 1012.45. HRMS-ESI-MS  $m/z$ : 1012.4516  $[\text{M-2Br}]^+$ ; calcd. for  $\text{C}_{66}\text{H}_{66}\text{N}_2\text{O}_4\text{P}_2$   $[\text{M-2Br}]^+$ : 1012.4492;  $m/z$ : 180.8263  $[\text{2Br+Na}]^-$ ; calcd. for  $\text{NaBr}_2$   $[\text{2Br+Na}]^-$ : 180.8270.

**1-2PF<sub>6</sub>.** 50 mg of 1-2Br (0.043 mmol) was dissolved in 5 mL of chloroform in a round-bottom flask. 278 mg of  $\text{NH}_4\text{PF}_6$  (1.70 mmol) was dissolved in 5 mL MeOH and added to the reaction mixture. The reaction mixture was allowed to stir overnight at room temperature and precipitated into 50 mL of DI water. The precipitate was filtered, washed with DI water and dried under

vacuum. Yield: 23 mg (41%). Off-white solid. Single crystals were obtained by layering diethyl ether on a concentrated solution of 1-PF<sub>6</sub> in acetonitrile. <sup>1</sup>H NMR (500 MHz, CDCl<sub>3</sub>) δ 8.33 (d, *J* = 14.1 Hz, 2H), 7.79 – 7.64 (m, 30H), 3.72 – 3.61 (m, 4H), 1.21 – 1.17 (m, 2H), 1.15 – 0.84 (m, 16H), 0.79 (t, *J* = 7.2 Hz, 6H), 0.57 (t, *J* = 7.4 Hz, 6H). <sup>13</sup>C{<sup>1</sup>H} NMR (125 MHz, CDCl<sub>3</sub>) δ 162.26, 160.96, 136.83, 136.72, 134.56, 133.79, 132.30, 131.91, 131.83, 130.53, 130.42, 128.33, 128.23, 125.94, 125.22, 120.74, 120.06, 45.18, 37.28, 30.21, 28.52, 23.06, 22.88, 14.23, 10.37. <sup>31</sup>P NMR (202 MHz, CDCl<sub>3</sub>) δ 31.06 (s, *PPh*<sub>3</sub>), -143.61 (hept, *J* = 711.5 Hz, *PF*<sub>6</sub>). <sup>19</sup>F NMR (470.39 MHz, CD<sub>3</sub>CN) δ -74.97, -76.41. <sup>19</sup>F NMR (470.39 MHz, CDCl<sub>3</sub>) δ -77.07, -78.59.

ESI-MS *m/z*: 1012.44 [M-2PF<sub>6</sub>]<sup>+</sup>; calcd. for C<sub>66</sub>H<sub>66</sub>N<sub>2</sub>O<sub>4</sub>P<sub>2</sub> [M-2PF<sub>6</sub>]<sup>+</sup>: 1012.45.

**1-2Cl.** 215 mg of 1-2Br (0.183 mmol) was dissolved in 5 mL of chloroform. 262 mg of silver chloride (1.830 mmol) and 5 mL of methanol were added and the suspension was sonicated in the dark for 30 mins. The suspension was allowed to stir overnight under light illumination. The reaction was filtered through 0.45 μm PTFE filter and solvent was removed using rotary evaporation. 20 mL of toluene was added to the residue and the mixture was sonicated for 10 mins. The mixture was filtered, washed with diethyl ether and vacuum dried. Yellow solid. Yield: 178 mg (89%). <sup>1</sup>H NMR (500 MHz, CDCl<sub>3</sub>) δ 8.36 (d, *J* = 13.6 Hz, 2H), 7.93 – 7.61 (m, 30H), 3.70 – 3.66 (m, 4H), 1.24 (br s, 2H), 1.11 – 0.86 (m, 16H), 0.78 (t, *J* = 6.6 Hz, 6H), 0.56 (br s, 6H). <sup>13</sup>C{<sup>1</sup>H} NMR (125 MHz, CDCl<sub>3</sub>) δ 162.48, 161.30, 137.02, 136.92, 134.45, 134.31, 133.27, 132.13, 132.05, 130.39, 130.28, 128.70, 128.61, 125.44, 124.73, 120.92, 120.14, 45.30, 37.38, 30.30, 28.46, 23.27, 23.02, 14.25, 10.39. <sup>31</sup>P NMR (202 MHz, CDCl<sub>3</sub>) δ 31.01.

ESI-MS *m/z*: 1012.45 [M-2Cl]<sup>+</sup>; calcd. for C<sub>66</sub>H<sub>66</sub>N<sub>2</sub>O<sub>4</sub>P<sub>2</sub> [M-2Cl]<sup>+</sup>: 1012.45.

**1-2NO<sub>3</sub>.** 200 mg of 1-Br (0.183 mmol) was dissolved in 10 mL of acetonitrile. 124.3 mg of silver nitrate (0.732 mmol) was added and the reaction was allowed to stir overnight under light illumination. The solvent was removed using rotary evaporation and 10 mL of chloroform was added. The suspension was filtered through 0.45 μm PTFE filter and solvent was removed using rotary evaporation. Yellow solids. Yield: 205 mg (99%). <sup>1</sup>H NMR (500 MHz, CDCl<sub>3</sub>) δ 8.35 (d, *J* = 14.1 Hz, 2H), 7.87 – 7.59 (m, 30H), 3.68 (m, 4H), 1.25 (br s, 2H), 1.18 – 0.83 (m, 16H), 0.79 (t, *J* = 7.1 Hz, 6H), 0.56 (t, *J* = 7.1 Hz, 6H). <sup>13</sup>C{<sup>1</sup>H} NMR (125 MHz, CDCl<sub>3</sub>) δ 162.37, 161.08, 136.85, 136.74, 134.51, 134.08, 132.75, 132.72, 131.34, 131.32, 131.26, 131.24, 130.39, 130.28,

128.28, 128.17, 125.66, 124.96, 120.86, 120.10, 45.27, 37.27, 30.19, 28.44, 23.05, 23.00, 14.25, 10.31.  $^{31}\text{P}$  NMR (202 MHz,  $\text{CDCl}_3$ )  $\delta$  31.02. ESI-MS  $m/z$ : 1012.24  $[\text{M}-2\text{NO}_3]^+$ ; calcd. for  $\text{C}_{66}\text{H}_{66}\text{N}_2\text{O}_4\text{P}_2$   $[\text{M}-2\text{NO}_3]^+$ : 1012.45.

**1-NO<sub>3</sub>**. 40 mg of **1-2NO<sub>3</sub>** (0.044 mmol) was dissolved in 10 mL of acetonitrile. 612.8  $\mu\text{L}$  of triethylamine was added and the reaction was allowed to stir for 10 mins. All the volatiles were removed using rotary evaporation and minimum acetonitrile was added to dissolve the residue, followed by precipitation in 200 mL of diethyl ether. The precipitate was filtered, washed with diethyl ether and vacuum dried. Dark-green solid. Yield: 20 mg (53%). ESI-MS  $m/z$ : 1012.23  $[\text{M}-\text{NO}_3]^+$ ; calcd. for  $\text{C}_{66}\text{H}_{66}\text{N}_2\text{O}_4\text{P}_2$   $[\text{M}-\text{NO}_3]^+$ : 1012.45.

1. All procedures were carried out in the glovebox. 100 mg of 1-Br (0.091 mmol) was dissolved in 4 mL of dry dichloromethane in a 20 mL glass vial. 10 mL of dry diethyl ether was carefully layered onto it. 0.5 mL of 1M  $\text{N}_2\text{H}_4$  in THF was carefully added to the diethyl ether layer. The vial was capped and kept undisturbed. After 3 days, crystals of single crystal quality were observed. The crystals were collected via filtration and washed with dry diethyl ether. Dark maroon solid. Yield: 44 mg (47%). ESI-MS  $m/z$ : 1012.23  $[\text{M}]^+$ ; calcd. for  $\text{C}_{66}\text{H}_{66}\text{N}_2\text{O}_4\text{P}_2$   $[\text{M}]^+$ : 1012.45.

## 2. X-ray crystallographic structures, selected crystal data, data collection, and refinement parameters

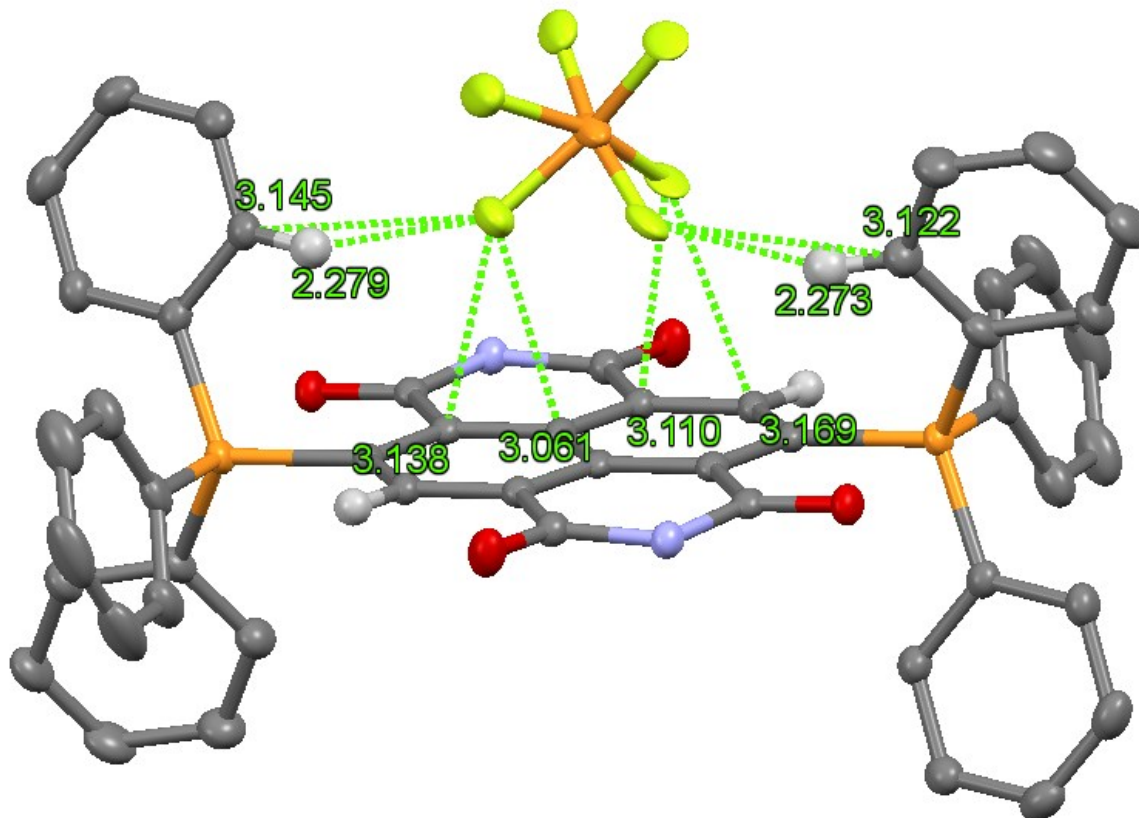


**Figure S1.** X-ray crystallographic structure of **1-PF<sub>6</sub>** showing PF<sub>6</sub><sup>-</sup> above the NDI core. Solvent molecules, alkyl groups and hydrogens on phenyl rings (except those with C-H...F short contacts) are omitted for clarity. [C-H...F] short contact distances: 2.279 and 2.273 Å, [C...F] short contact distances: 3.061, 3.110, 3.044, 3.138 and 3.169 Å.

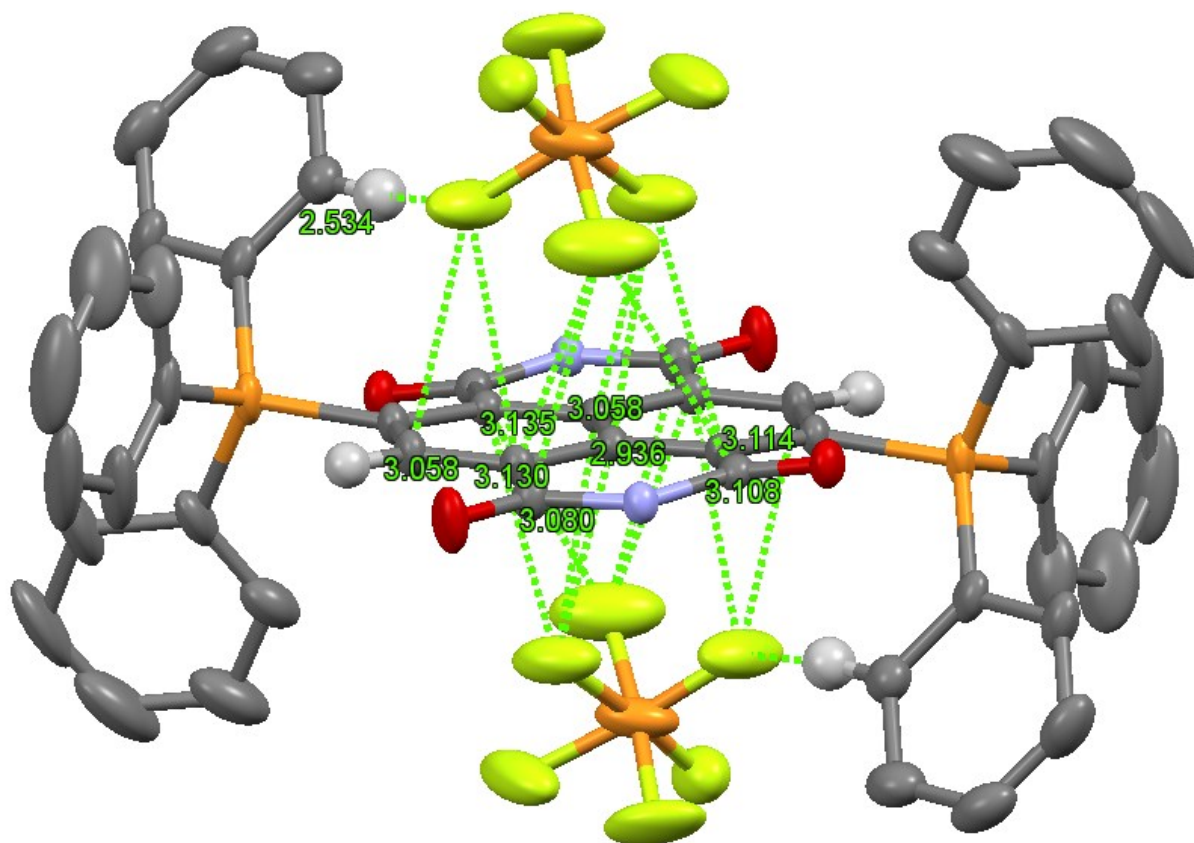


**Figure S2.** X-ray crystallographic structure of **1-2PF<sub>6</sub>** showing PF<sub>6</sub><sup>-</sup> above and below the NDI core. Alkyl groups and hydrogens on phenyl rings (except those with C–H•••F short contacts) are omitted for clarity. Short contact distances shown for the top PF<sub>6</sub> as the bottom PF<sub>6</sub> ion is a mirror image of the top PF<sub>6</sub>. [C–H•••F] short contact distances: 2.534 Å, [C•••F] short contact distances: 2.936, 3.058, 3.080, 3.108, 3.114, 3.130 and 3.135 Å.

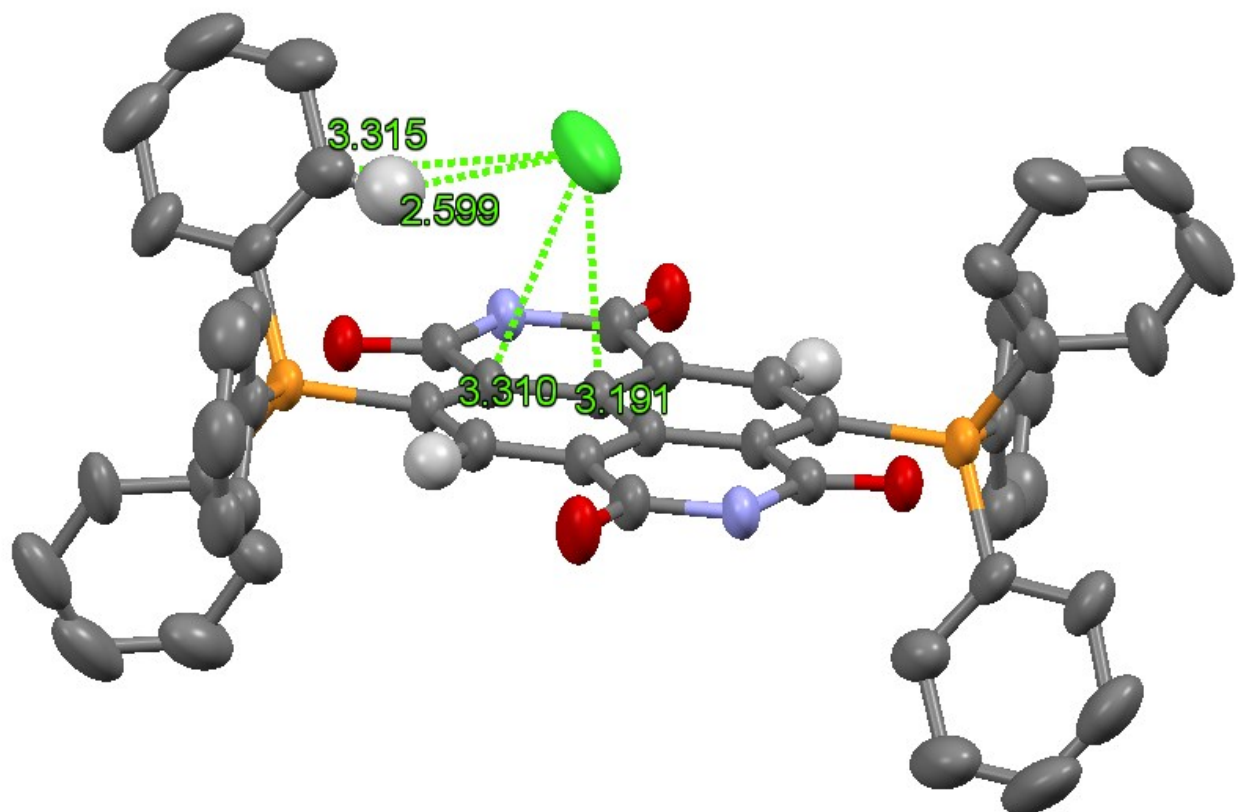


**Figure S3.** X-ray crystallographic structure of **1-Cl** showing  $\text{Cl}^-$  above the NDI core. Solvent molecules, alkyl groups and hydrogens on phenyl rings (except those with  $\text{C-H}\cdots\text{Cl}^-$  short contacts) are omitted for clarity.  $[\text{C-H}\cdots\text{Cl}^-]$  short contact distances: 2.599 Å,  $[\text{C}\cdots\text{Cl}^-]$  short contact distances: 3.191, 3.310 and 3.315 Å.

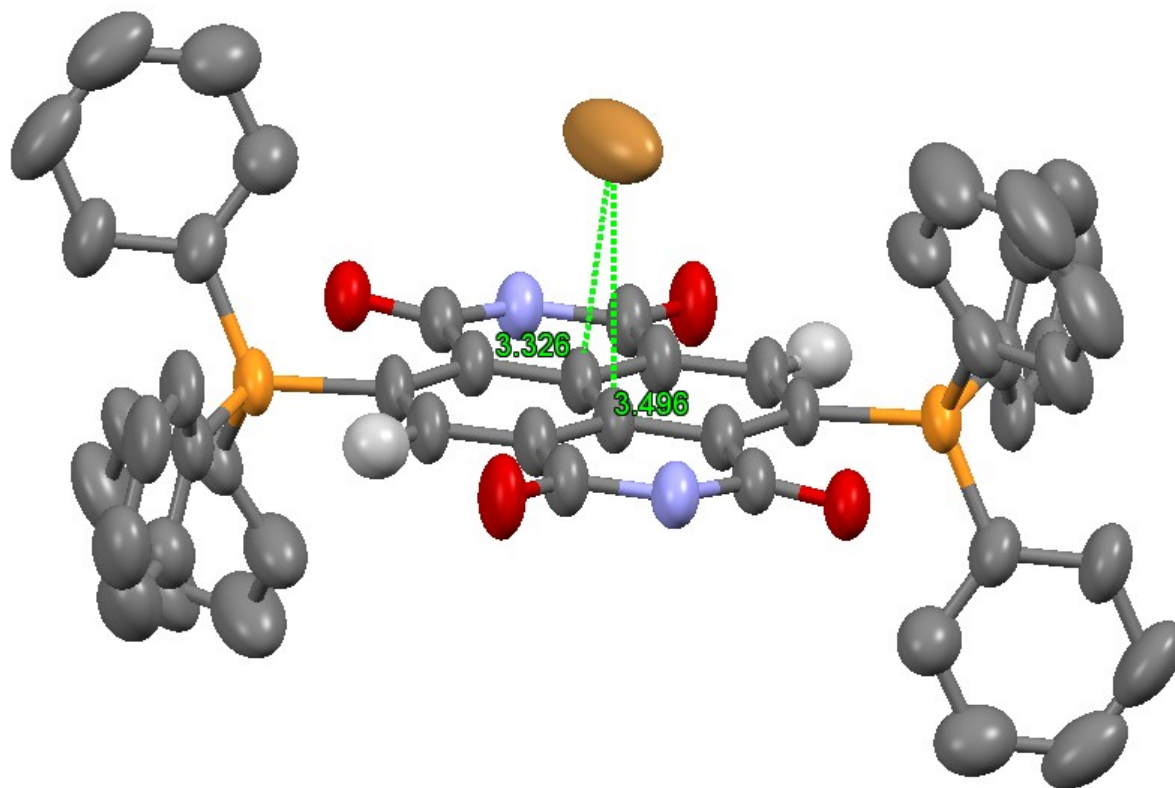


**Figure S4.** X-ray crystallographic structure of **1-Br** showing  $\text{Br}^-$  above the NDI core. Solvent molecules, alkyl groups and hydrogens on phenyl rings are omitted for clarity.  $[\text{C}\cdots\text{Br}^-]$  short contact distances: 3.326 and 3.496 Å.

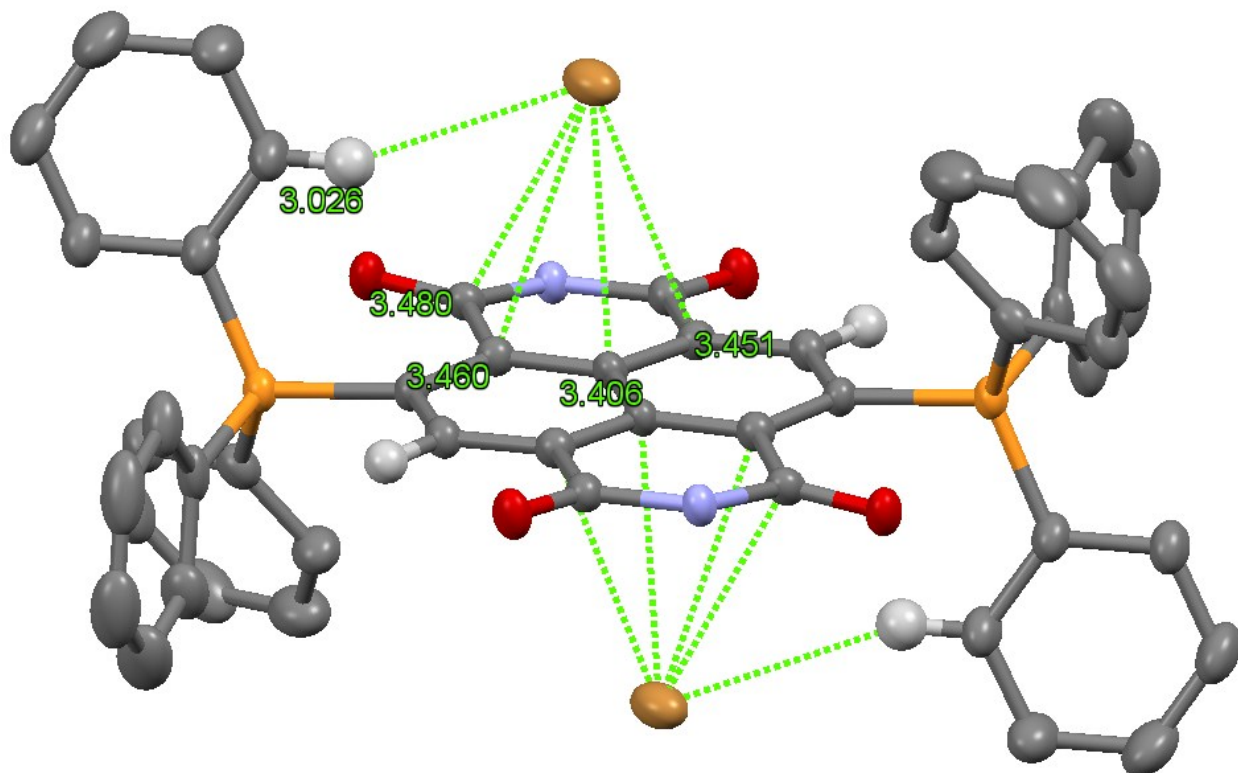


**Figure S5.** X-ray crystallographic structure of **1-2Br** showing  $\text{Br}^-$  above and below the NDI core. Alkyl groups and hydrogens on phenyl rings (except those with  $\text{C-H}\cdots\text{Br}^-$  short contacts) are omitted for clarity. Short contact distances shown for the top  $\text{Br}^-$  as the bottom  $\text{Br}^-$  is a mirror image of the top  $\text{Br}^-$ .  $[\text{C-H}\cdots\text{Br}^-]$  short contact distances: 3.026 Å,  $[\text{C}\cdots\text{Br}^-]$  short contact distances: 3.406, 3.451, 3.460 and 3.480 Å.

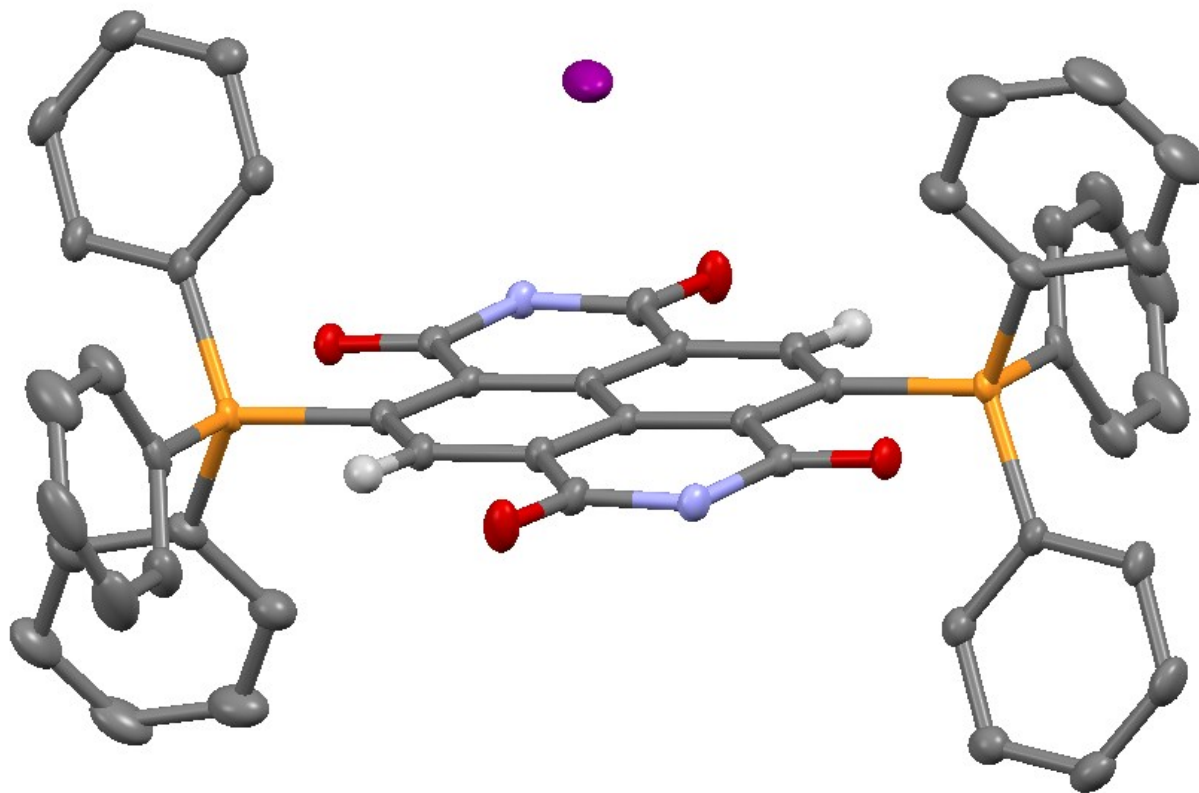


**Figure S6.** X-ray crystallographic structure of **1-I** showing  $\text{I}^-$  above the NDI core. Solvent molecules, alkyl groups and hydrogens on phenyl rings are omitted for clarity. There are no  $[\text{C}\cdots\text{H}\cdots\text{I}^-]$  and  $[\text{C}\cdots\text{I}^-]$  short contacts.

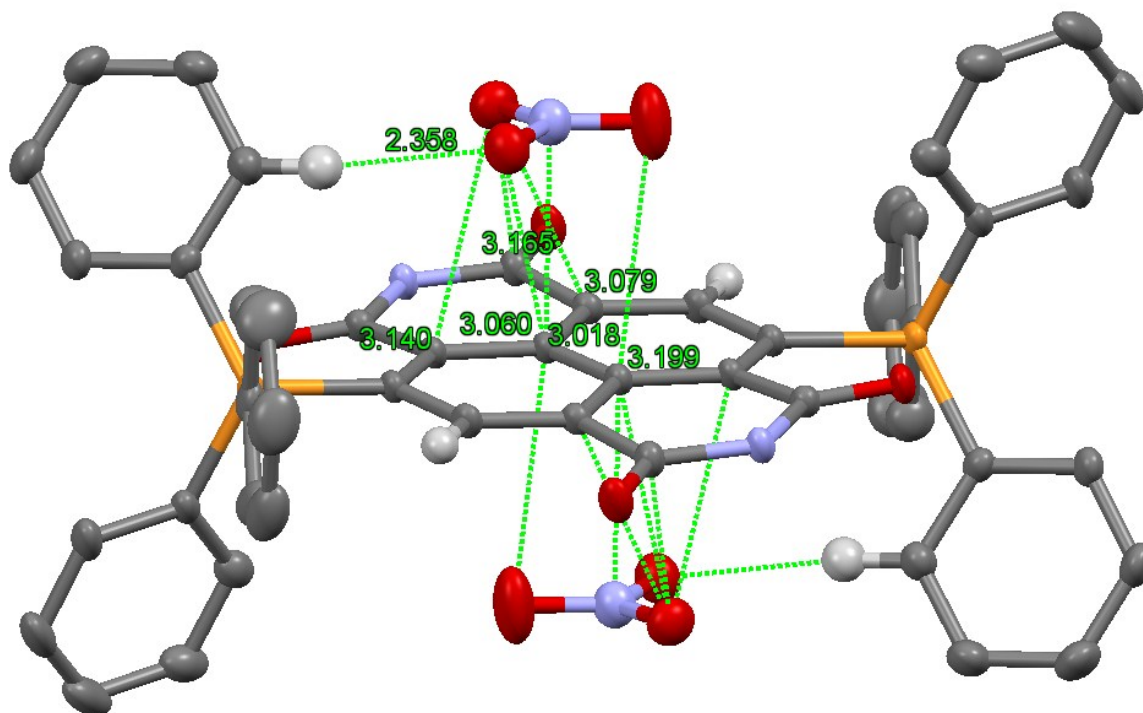


**Figure S7.** X-ray crystallographic structure of **1-2NO<sub>3</sub>** showing NO<sub>3</sub><sup>-</sup> above and below the NDI core. Alkyl groups and hydrogens on phenyl rings (except those with C–H•••O short contacts) are omitted for clarity. Short contact distances shown for the top NO<sub>3</sub><sup>-</sup> as the bottom NO<sub>3</sub><sup>-</sup> is a mirror image of the top NO<sub>3</sub><sup>-</sup>. [C–H•••O] short contact distances: 2.358 Å, [C•••O] short contact distances: 3.060, 3.079, 3.140, 3.165 and 3.199 Å. [N•••O] short contact distances: 3.018 Å.

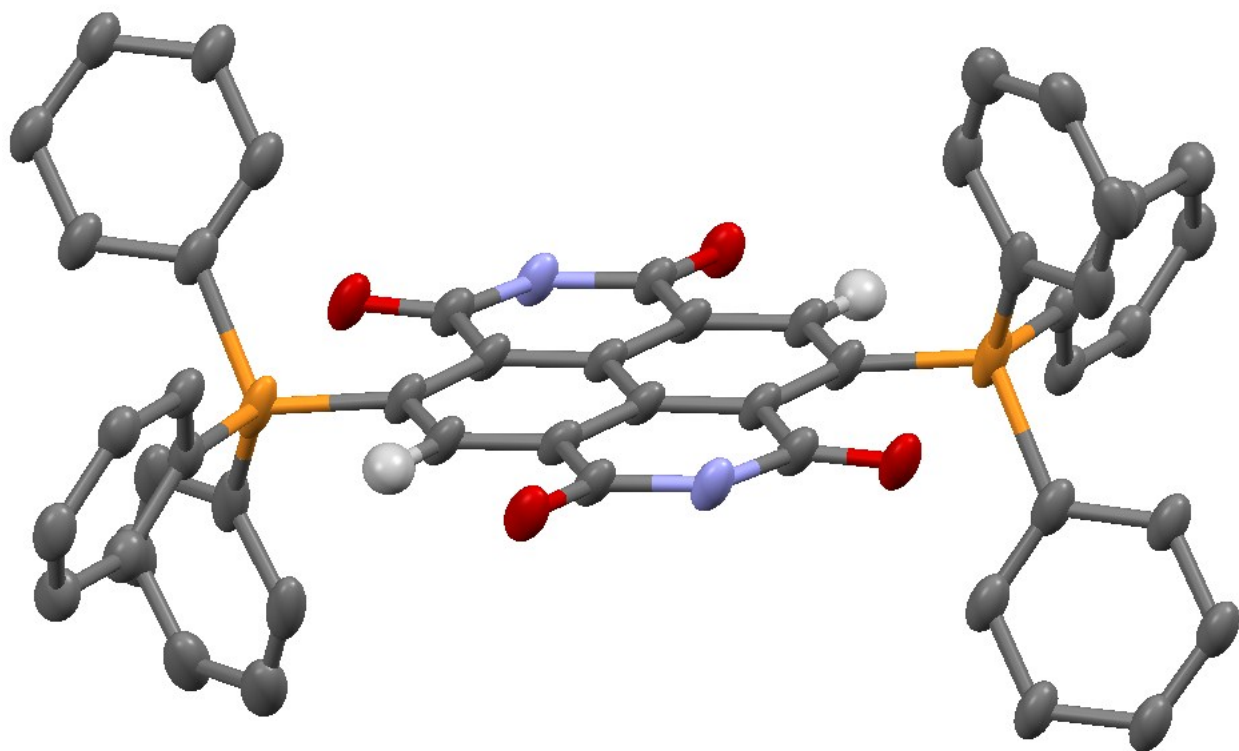


**Figure S8.** X-ray crystallographic structure of **1**. Alkyl groups and hydrogens on phenyl rings are omitted for clarity.

	<b>1-Br</b>	<b>1-2Br</b>	<b>1-I</b>	<b>1-2NO<sub>3</sub></b>
Empirical formula	C <sub>66</sub> H <sub>66</sub> BrN <sub>2</sub> O <sub>4</sub> P <sub>2</sub>	C <sub>34</sub> H <sub>33</sub> BrCl <sub>3</sub> NO <sub>2</sub> P	C <sub>66</sub> H <sub>66</sub> IN <sub>2</sub> O <sub>4</sub> P <sub>2</sub>	C <sub>68</sub> H <sub>68</sub> Cl <sub>6</sub> N <sub>4</sub> O <sub>10</sub> P <sub>2</sub>
Formula weight	1095.72	705.85	1140.04	1375.90
Temperature of data collection	100(2) K	100(2) K	100(2) K	101(2) K
Wavelength	1.54178 Å	1.54178 Å	0.71073 Å	1.54178 Å
Crystal size	0.147 x 0.217 x 0.242 mm <sup>3</sup>	0.140 x 0.169 x 0.188 mm <sup>3</sup>	0.161 x 0.070 x 0.068 mm <sup>3</sup>	0.236 x 0.225 x 0.122 mm <sup>3</sup>
Crystal system	Trigonal	Monoclinic	Monoclinic	Trigonal
Space group	R -3	P 1 2 <sub>1</sub> /c 1	C2/c	R -3
Unit cell dimensions	a = 24.7543(7) Å α = 90° b = 24.7543(7) Å β = 90° c = 30.0212(9) Å γ = 120°	a = 10.9670(6) Å α = 90° b = 15.8648(10) Å β = 105.084(3)° c = 20.3172(11) Å γ = 90°	a = 19.7346(13) Å α = 90° b = 19.9943(12) Å β = 110.360(2)° c = 14.9829(7) Å γ = 90°	a = 25.2081(12) Å α = 90° b = 25.2081(12) Å β = 90° c = 30.1100(16) Å γ = 120°
Volume	15931.6(12) Å <sup>3</sup>	3413.2(3) Å <sup>3</sup>	5542.6(6)	16570.0(18) Å <sup>3</sup>
Z	9	4	4	9
Density (calculated)	1.028 g/cm <sup>3</sup>	1.374 g/cm <sup>3</sup>	1.366 g/cm <sup>3</sup>	1.241 g/cm <sup>3</sup>
F(000)	5168	1448	2364	6444
Theta range for data collection	3.60 to 67.68°	3.58 to 75.44°	2.900 to 28.339°	2.500 to 66.595°
Reflections collected	89076	24969	28147	45452
Independent reflections	6700	6662 [R(int) = 0.0421]	6877 [R(int) = 0.0356]	6508 [R(int) = 0.0428]
Goodness-of-fit on F <sup>2</sup>	2.005	1.042	1.039	0.996
Final R indices [I > 2σ(I)]	R1 = 0.1345 wR2 = 0.3998	R1 = 0.0630, wR2 = 0.1632	R1 = 0.0566, wR2 = 0.1493	R1 = 0.0656, wR2 = 0.1913
R indices (all data)	R1 = 0.1455, wR2 = 0.4175	R1 = 0.0818, wR2 = 0.1801	R1 = 0.0664, wR2 = 0.1555	R1 = 0.0688, wR2 = 0.1949
Largest diff. peak and hole	1.929 and -0.509 e.Å <sup>-3</sup>	1.233 and -0.643 e.Å <sup>-3</sup>	2.710 and -1.072 e.Å <sup>-3</sup>	1.136 and -0.981 e.Å <sup>-3</sup>

**Table S1.** Selected crystal data, data collection, and refinement parameters for **1-Br**, **1-2Br**, **1-I** and **1-2NO<sub>3</sub>**.

	<b>1-PF<sub>6</sub></b>	<b>1-2PF<sub>6</sub></b>	<b>1-Cl</b>	<b>1</b>
Empirical formula	C <sub>66</sub> H <sub>66</sub> F <sub>6</sub> N <sub>2</sub> O <sub>4</sub> P <sub>3</sub>	C <sub>74</sub> H <sub>86</sub> F <sub>12</sub> N <sub>2</sub> O <sub>6</sub> P <sub>4</sub>	C <sub>66</sub> H <sub>66</sub> ClN <sub>2</sub> O <sub>7.33</sub> P <sub>2</sub>	C <sub>66</sub> H <sub>66</sub> N <sub>2</sub> O <sub>4</sub> P <sub>2</sub>
Formula weight	1158.11	1451.32	1101.93	1013.14
Temperature of data collection	100(2) K	100(2) K	100(2) K	100(2) K
Wavelength	1.54178 Å	1.54178 Å	1.54178 Å	1.54178 Å
Crystal size	0.346 x 0.077 x 0.073 mm <sup>3</sup>	0.346 x 0.181 x 0.072 mm <sup>3</sup>	0.389 x 0.285 x 0.217 mm <sup>3</sup>	0.218 x 0.182 x 0.079 mm <sup>3</sup>
Crystal system	Monoclinic	Orthorhombic	Trigonal	Monoclinic
Space group	C2/c	Pbca	R-3	P2 <sub>1</sub> /c
Unit cell dimensions	a = 19.6640(5) Å α = 90° b = 19.9512(6) Å β = 111.1250(10)° c = 15.5025(4) Å γ = 90°	a = 15.5817(5) Å α = 90° b = 20.6208(6) Å β = 90° c = 22.0566(7) Å γ = 90°	a = 24.8062(9) Å α = 90° b = 24.8062(9) Å β = 90° c = 30.0418(11) Å γ = 120°	a = 14.2234(9) Å α = 90° b = 15.5567(11) Å β = 108.744(2)° c = 12.5242(8) Å γ = 90°
Volume	5673.2(3) Å <sup>3</sup>	7086.9(4) Å <sup>3</sup>	16009.5(13) Å <sup>3</sup>	2624.2(3) Å <sup>3</sup>
Z	4	4	9	2
Density (calculated)	1.356 g/cm <sup>3</sup>	1.360 g/cm <sup>3</sup>	1.029 g/cm <sup>3</sup>	1.282 g/cm <sup>3</sup>
F(000)	2428	3040	5235	1076
Theta range for data collection	3.841 to 70.162°	4.008 to 66.587°	2.528 to 66.594°	4.342 to 66.676°
Reflections collected	24255	76842	49333	25696
Independent reflections	5281 [R(int) = 0.0469]	6224 [R(int) = 0.0419]	6201 [R(int) = 0.0443]	4621 [R(int) = 0.0386]
Goodness-of-fit on F <sup>2</sup>	1.066	1.046	2.015	1.119
Final R indices [I>2σ(I)]	R1 = 0.0565, wR2 = 0.1540	R1 = 0.1029, wR2 = 0.2711	R1 = 0.1377, wR2 = 0.4022	R1 = 0.0711, wR2 = 0.2076
R indices (all data)	R1 = 0.0587, wR2 = 0.1587	R1 = 0.1075, wR2 = 0.2756	R1 = 0.1453, wR2 = 0.4169	R1 = 0.0775, wR2 = 0.2176
Largest diff. peak and hole	0.638 and -0.640 e.Å <sup>-3</sup>	1.353 and -0.758 e.Å <sup>-3</sup>	1.495 and -0.758 e.Å <sup>-3</sup>	1.149 and -0.881 e.Å <sup>-3</sup>

**Table S2.** Selected crystal data, data collection, and refinement parameters for **1-PF<sub>6</sub>**, **1-2PF<sub>6</sub>**, **1-Cl** and **1**.

### 3. Characterization data of DTPP-NDI salts

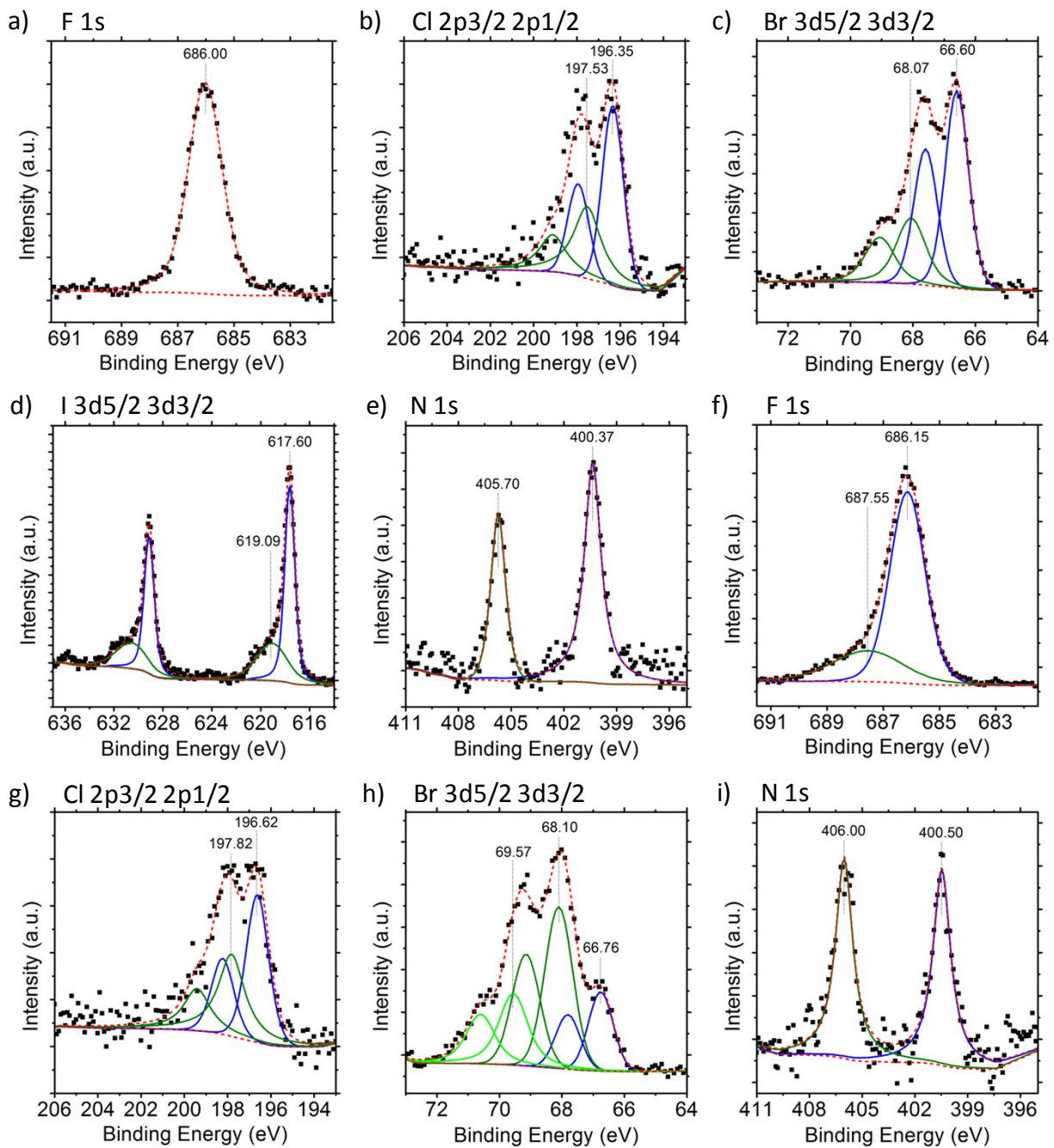


**Figure S9.** XPS spectra of a) **1-PF<sub>6</sub>**, b) **1-Cl**, c) **1-Br**, d) **1-I**, e) **1-NO<sub>3</sub>**, f) **1-2PF<sub>6</sub>**, g) **1-2Cl**, h) **1-2Br** and i) **1-2NO<sub>3</sub>**.

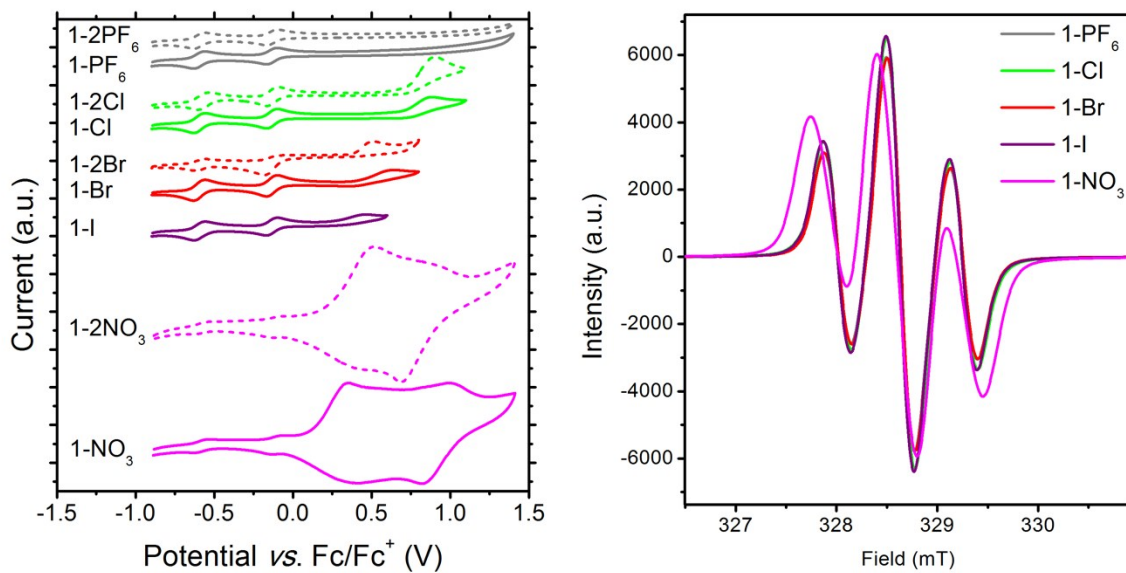


**Figure S10.** Cyclic voltammogram of the 1+ and 2+ salts in dry acetonitrile and right) EPR of the 1+ salts in dry dichloromethane.

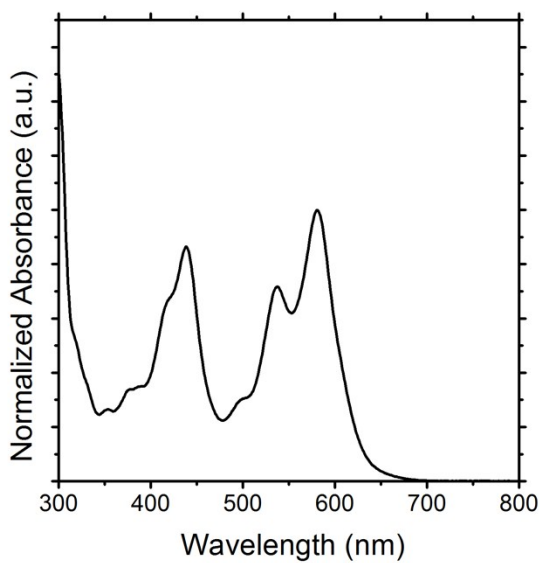


**Figure S11.** Solution UV-Vis absorption of **1** in dry THF.

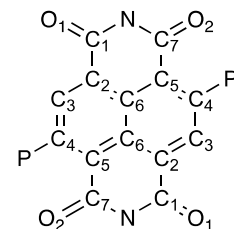
	Cation	$\delta$ of Anion (ppm)	LW <sub>1/2</sub> (Hz)
PF <sub>6</sub> <sup>-</sup> ( <sup>19</sup> F) Acetonitrile- <i>d</i> <sub>3</sub>	TBA	-74.82, -76.32	1.5
	1+	-74.78, -76.28	1.9
	2+	-74.91, -76.41	1.5
PF <sub>6</sub> <sup>-</sup> ( <sup>19</sup> F) Chloroform- <i>d</i>	TBA	-75.14, -76.65	1.5
	1+	-76.13, -77.65	162.5
	2+	-77.07, -78.59	4.4
Cl <sup>-</sup> ( <sup>35</sup> Cl) Acetonitrile- <i>d</i> <sub>3</sub>	TBA	40.18	11
	1+	37.89	63
	2+	Not observed	-
Cl <sup>-</sup> ( <sup>35</sup> Cl) Chloroform- <i>d</i>	TBA	3.49	259
	1+	-2.26	415
	2+	Not observed	-
Br <sup>-</sup> ( <sup>81</sup> Br) Acetonitrile- <i>d</i> <sub>3</sub>	TBA	83.43	178
	1+	86.32	915
	2+	Not observed	-
Br <sup>-</sup> ( <sup>81</sup> Br) Chloroform- <i>d</i>	TBA	Not observed	-
	1+	Not observed	-
	2+	Not observed	-

**Table S3.** Halogen NMR for BTPP-NDI salts.  $\delta$ : Chemical shift, LW<sub>1/2</sub>: linewidth at half peak height. No <sup>127</sup>I signal could be observed for **1-I** in both acetonitrile-*d*<sub>3</sub> and chloroform-*d*.

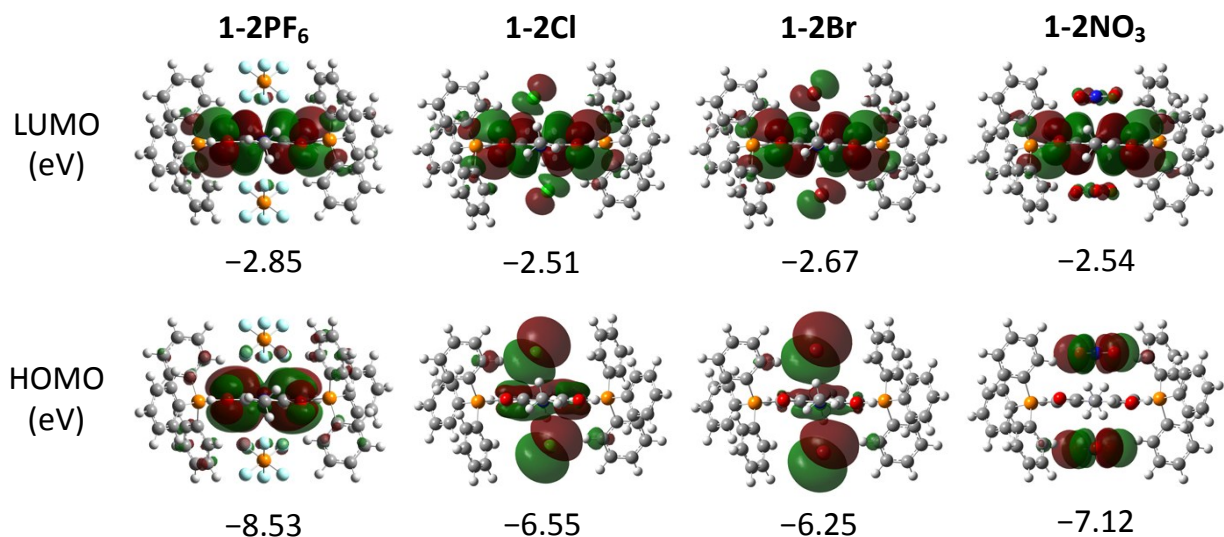
### Density Functional Theory Calculation

All calculations were carried out using Gaussian 09 package. 1 was geometry optimized using CAM-B3LYP 6-311+(d,p) level of theory in the gas phase in  $C_i$  symmetry. The 2+ salts were geometry optimized using CAM-B3LYP 6-311+(d,p) for the atoms in the cation and LANL2DZPD for the atoms in the anion in the gas phase in  $C_i$  symmetry. For the 1+ salts, the structures were first optimized using CAM-B3LYP 6-311+(d,p) for the atoms in the cation and LANL2DZPD for the atoms in the anion in the gas phase having  $C_i$  symmetry by adding an additional anion, with the overall charge of the molecule as -1. Single-point calculation was then carried out on the optimized geometry with the additional anion removed (hence overall charge neutral) to obtain the molecular orbitals and spin densities. Single-point time-dependent DFT calculation was carried out using the optimized structures. Keywords pseudo=read and guess=mix were used for all calculations.

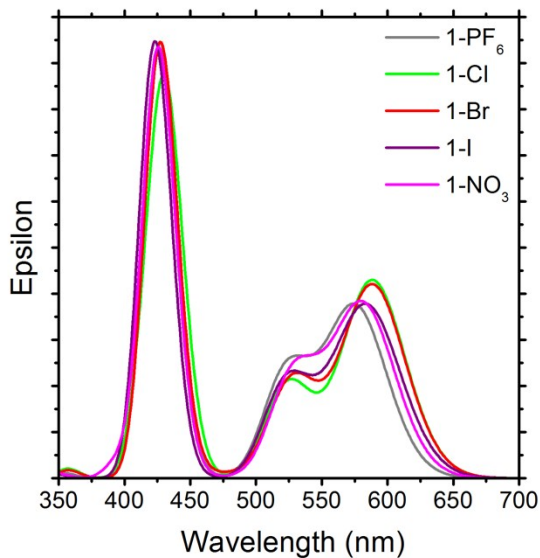
**Table S4.** NDI core bond lengths from single crystal (expt.) and DFT geometry optimized (calc.) structures. <sup>a</sup> distance from the NDI plane to the nearest atom in the anion for **1-PF<sub>6</sub>**, **1-2PF<sub>6</sub>**, **1-NO<sub>3</sub>** and **1-2NO<sub>3</sub>**.



		<b>1</b>	<b>1-PF<sub>6</sub></b>	<b>1-Cl</b>	<b>1-Br</b>	<b>1-I</b>	<b>1-NO<sub>3</sub></b>	<b>1-2PF<sub>6</sub></b>	<b>1-2Cl</b>	<b>1-2Br</b>	<b>1-2NO<sub>3</sub></b>
O <sub>1</sub> -C <sub>1</sub>	Expt.	1.240	1.228	1.224	1.228	1.227	N.A.	1.209	N.A.	1.216	1.215
	Calc.	1.228	1.251	1.249	1.249	1.250	1.252	1.237	1.238	1.237	1.236
	Dev.	+0.012	-0.023	-0.025	-0.021	-0.023	N.A.	-0.028	N.A.	-0.021	-0.021
	% Dev.	0.97	1.87	2.04	1.71	1.87	N.A.	2.32	N.A.	1.73	1.73
C <sub>1</sub> -C <sub>2</sub>	Expt.	1.441	1.456	1.443	1.453	1.452	N.A.	1.490	N.A.	1.482	1.479
	Calc.	1.443	1.450	1.454	1.453	1.450	1.449	1.474	1.474	1.474	1.472
	Dev.	-0.002	+0.006	-0.011	0	+0.002	N.A.	+0.016	N.A.	+0.008	+0.007
	% Dev.	0.14	0.41	0.76	0	0.14	N.A.	1.07	N.A.	0.54	0.47
C <sub>2</sub> -C <sub>3</sub>	Expt.	1.406	1.394	1.396	1.393	1.391		1.370	N.A.	1.370	1.373
	Calc.	1.409	1.393	1.394	1.394	1.392	1.393	1.370	1.371	1.371	1.369
	Dev.	-0.003	+0.001	+0.002	-0.001	-0.001	N.A.	0	N.A.	-0.001	+0.004
	% Dev.	0.21	0.07	0.14	0.07	0.07	N.A.	0	N.A.	0.07	0.29
C <sub>3</sub> -C <sub>4</sub>	Expt.	1.377	1.387	1.389	1.387	1.389	N.A.	1.414	N.A.	1.413	1.409
	Calc.	1.372	1.382	1.386	1.385	1.381	1.380	1.405	1.408	1.407	1.404
	Dev.	+0.005	+0.005	+0.003	+0.002	+0.008	N.A.	+0.009	N.A.	+0.006	+0.005
	% Dev.	0.36	0.36	0.22	0.14	0.58	N.A.	0.64	N.A.	0.42	0.35
C <sub>4</sub> -C <sub>5</sub>	Expt.	1.454	1.430	1.413	1.428	1.416	N.A.	1.387	N.A.	1.394	1.397
	Calc.	1.453	1.413	1.413	1.413	1.414	1.413	1.382	1.382	1.383	1.381
	Dev.	+0.001	+0.017	0	+0.015	+0.002	N.A.	+0.005	N.A.	+0.011	+0.016
	% Dev.	0.07	1.19	0	1.05	0.14	N.A.	0.36	N.A.	0.79	1.15
C <sub>5</sub> -C <sub>6</sub>	Expt.	1.398	1.405	1.409	1.400	1.405	N.A.	1.408	N.A.	1.405	1.408
	Calc.	1.394	1.402	1.401	1.402	1.402	1.401	1.409	1.410	1.410	1.409
	Dev.	+0.004	+0.003	+0.008	-0.002	+0.003	N.A.	-0.001	N.A.	-0.005	-0.01
	% Dev.	0.29	0.21	0.57	0.14	0.21	N.A.	0.07	N.A.	0.36	0.71
C <sub>6</sub> -C <sub>6</sub>	Expt.	1.433	1.421	1.422	1.413	1.411	N.A.	1.412	N.A.	1.406	1.406
	Calc.	1.437	1.421	1.420	1.420	1.422	1.421	1.405	1.401	1.402	1.406
	Dev.	-0.004	0	+0.002	-0.007	-0.011	N.A.	+0.007	N.A.	+0.004	0
	% Dev.	0.28	0	0.14	0.50	0.78	N.A.	0.50	N.A.	0.28	0
C <sub>2</sub> -C <sub>6</sub>	Expt.	1.419	1.410	1.405	1.424	1.409	N.A.	1.405	N.A.	1.412	1.408
	Calc.	1.414	1.409	1.410	1.409	1.408	1.408	1.406	1.407	1.407	1.407
	Dev.	+0.005	+0.001	-0.005	+0.015	+0.001	N.A.	-0.001	N.A.	+0.005	+0.001
	% Dev.	0.35	0.07	0.36	1.05	0.07	N.A.	0.07	N.A.	0.35	0.07
C <sub>5</sub> -C <sub>7</sub>	Expt.	1.423	1.446	1.454	1.443	1.449	N.A.	1.478	N.A.	1.476	1.482
	Calc.	1.425	1.440	1.441	1.442	1.441	1.439	1.473	1.473	1.473	1.472
	Dev.	-0.002	+0.006	+0.013	+0.001	+0.008	N.A.	+0.005	N.A.	+0.003	+0.01
	% Dev.	0.14	0.41	0.89	0.07	0.55	N.A.	0.33	N.A.	0.20	0.67
O <sub>2</sub> -C <sub>7</sub>	Expt.	1.249	1.237	1.236	1.231	1.234	N.A.	1.218	N.A.	1.221	1.221
	Calc.	1.245	1.264	1.264	1.264	1.264	1.264	1.246	1.247	1.247	1.247
	Dev.	+0.004	-0.027	-0.028	-0.033	-0.030	N.A.	-0.028	N.A.	-0.014	-0.026
	% Dev.	0.32	2.18	2.27	2.68	2.43	N.A.	2.30	N.A.	1.14	2.13
N-C <sub>7</sub>	Expt.	1.397	1.393	1.384	1.399	1.389	N.A.	1.390	N.A.	1.394	1.390
	Calc.	1.384	1.379	1.375	1.376	1.380	1.381	1.376	1.375	1.375	1.376
	Dev.	+0.013	+0.014	+0.009	+0.023	+0.009	N.A.	+0.014	N.A.	+0.019	+0.014
	% Dev.	0.93	1.01	0.65	1.64	0.65	N.A.	1.01	N.A.	1.36	1.01
N-C <sub>1</sub>	Expt.	1.406	1.404	1.408	1.403	1.391	N.A.	1.393	N.A.	1.394	1.398
	Calc.	1.409	1.402	1.400	1.401	1.403	1.403	1.397	1.395	1.396	1.399
	Dev.	-0.003	+0.002	+0.008	+0.002	-0.012	N.A.	-0.004	N.A.	-0.002	-0.001
	% Dev.	0.21	0.14	0.57	0.14	0.86	N.A.	0.29	N.A.	0.14	0.07
P-C <sub>4</sub>	Expt.	1.781	1.792	1.812	1.797	1.786	N.A.	1.822	N.A.	1.827	1.822
	Calc.	1.780	1.837	1.844	1.843	1.833	1.833	1.862	1.864	1.862	1.857
	Dev.	+0.001	-0.045	-0.032	-0.046	-0.047	N.A.	-0.040	N.A.	-0.035	-0.035
	% Dev.	0.06	2.51	1.77	2.56	2.63	N.A.	2.20	N.A.	1.92	1.92
X <sup>-</sup> ·π	Expt.	-	2.914	3.147	3.315	3.761	N.A.	2.806	N.A.	3.197	2.834
	Calc.	-	3.026	3.320	3.568	4.041	2.933	2.796	2.939	3.189	2.964
	Dev.	-	-0.112	-0.173	-0.253	-0.280	N.A.	+0.01	N.A.	+0.008	-0.13
	% Dev.	-	3.84	5.50	7.63	7.44	N.A.	0.36	N.A.	0.25	4.59

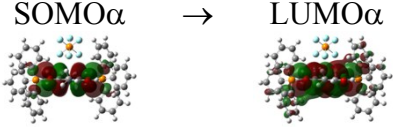
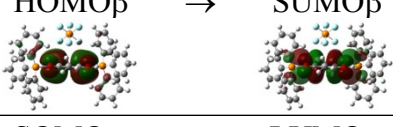
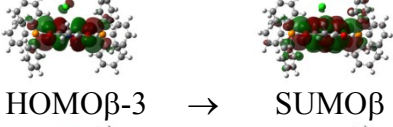
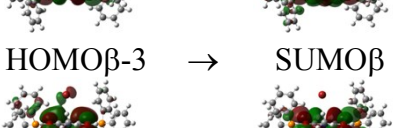
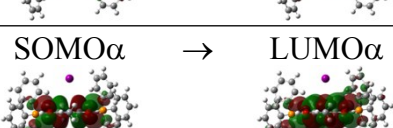
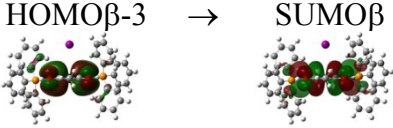
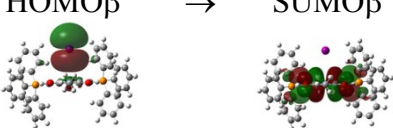
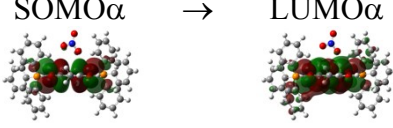
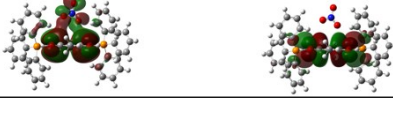


**Figure S12.** Frontier molecular orbitals ( $0.01 e^-/\text{au}^3$ ) of the geometry optimized 2+ salts in the gas phase using DFT RCAMB3LYP 6-311G+ (d,p) for atoms in cation and LANL2DZ with polarization and diffuse functions for atoms in anion.



**Figure S13.** Time dependant DFT calculated UV-Vis absorption of the 1+ salts in chloroform. Number of states calculated = 10. Largest absorption peak shift due to change of anion corresponds to  $\lambda_{\text{max}}$ , which is in agreement with the experimental solution UV-Vis absorption.

**Table S5.** TDDFT calculation of the  $D_0 \rightarrow D_1$  transition ( $\lambda_{\max}$ ) for the 1+ salts using IEFPCM in chloroform. Molecular orbitals were shown using isovalue of  $0.01 \text{ e}^-/\text{au}^3$ .

Compound	Wavelength	Oscillator strength	Molecular orbitals involved	CIS coefficient
1-PF <sub>6</sub>	576 nm (2.15 eV)	0.1357	SOMO $\alpha$ → LUMO $\alpha$ 	0.93408
			HOMO $\beta$ → SUMO $\beta$ 	0.27287
1-Cl	589 nm (2.11 eV)	0.1585	SOMO $\alpha$ → LUMO $\alpha$ 	0.95347
			HOMO $\beta$ -3 → SUMO $\beta$ 	-0.18745
1-Br	589 nm (2.11 eV)	0.1546	SOMO $\alpha$ → LUMO $\alpha$ 	0.95210
			HOMO $\beta$ -3 → SUMO $\beta$ 	-0.19634
1-I	590 nm (2.10 eV)	0.0881	SOMO $\alpha$ → LUMO $\alpha$ 	0.76926
			HOMO $\beta$ -3 → SUMO $\beta$ 	0.13325
			HOMO $\beta$ → SUMO $\beta$ 	-0.59239
1-NO <sub>3</sub>	582 nm (2.13 eV)	0.1375	SOMO $\alpha$ → LUMO $\alpha$ 	0.94420
			HOMO $\beta$ -1 → SUMO $\beta$ 	0.22969

#### 4. $^1\text{H}$ , $^{13}\text{C}\{^1\text{H}\}$ NMR and ESI mass spectra of synthesized compounds

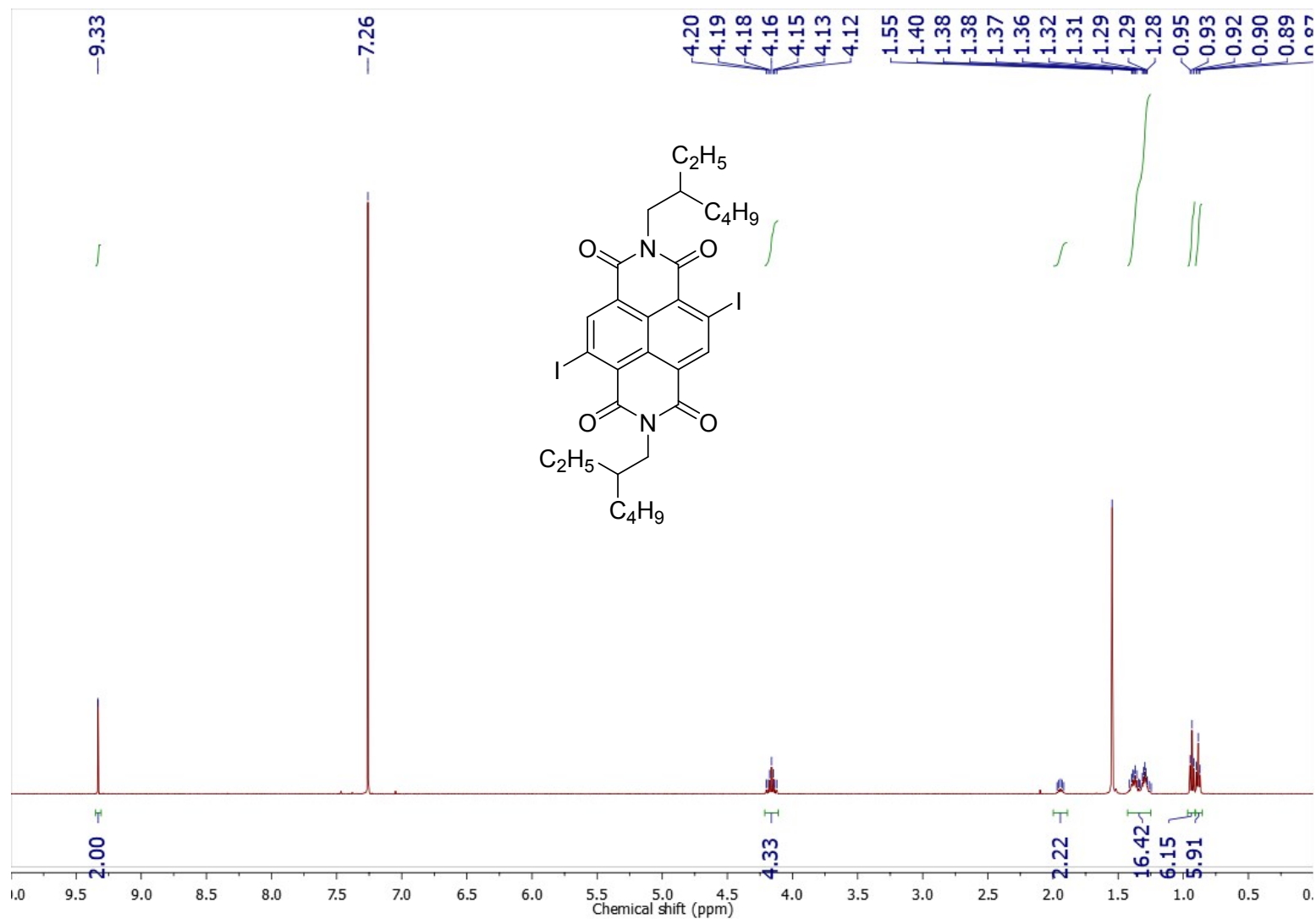


**Figure S14.**  $^1\text{H}$  NMR spectrum (500 MHz) of  $\text{I}_2\text{-NDI}$  in  $\text{CDCl}_3$ .

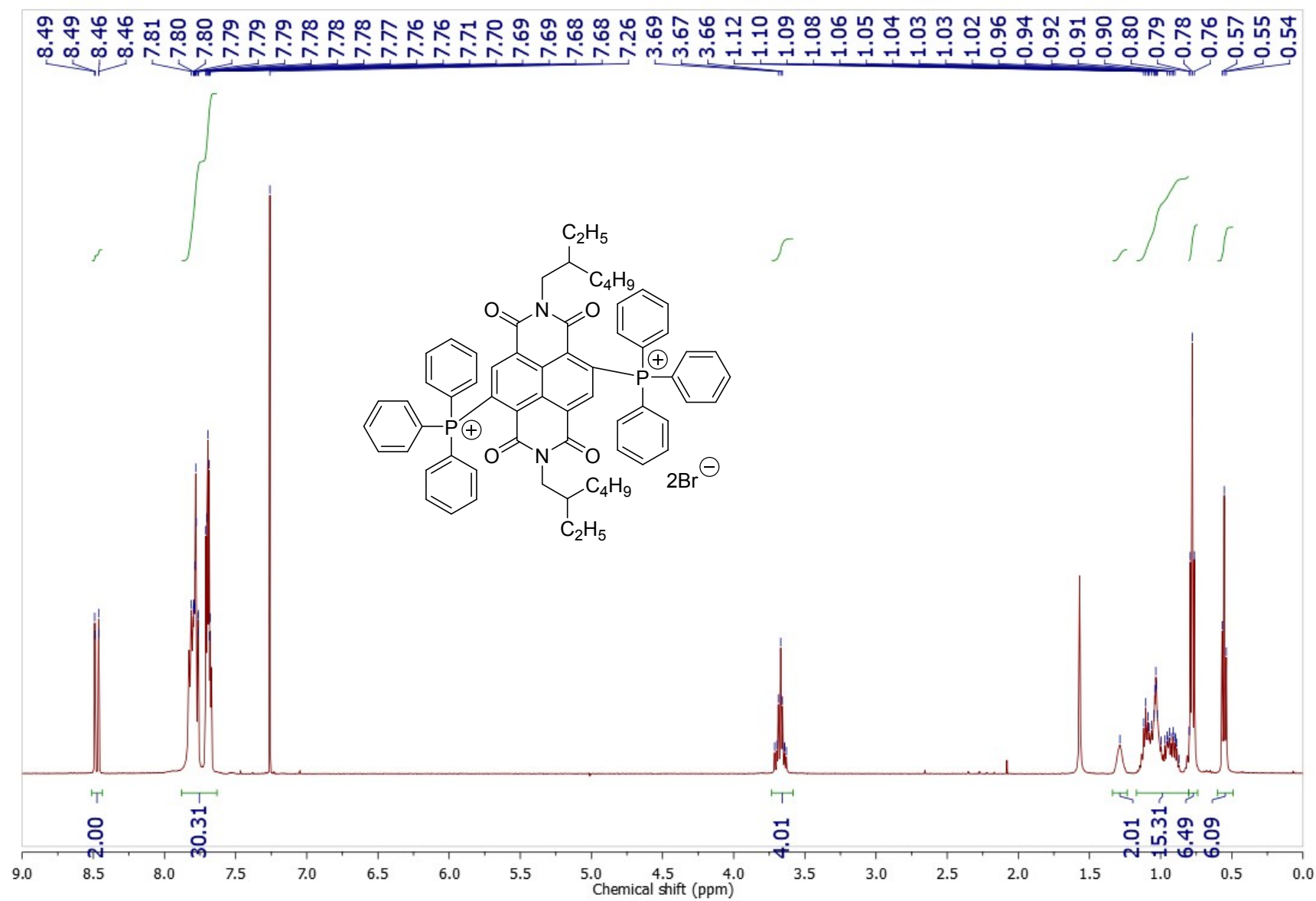


**Figure S15.** <sup>1</sup>H NMR spectrum (500 MHz) of **1-2Br** in DMSO-*d*<sub>6</sub>.

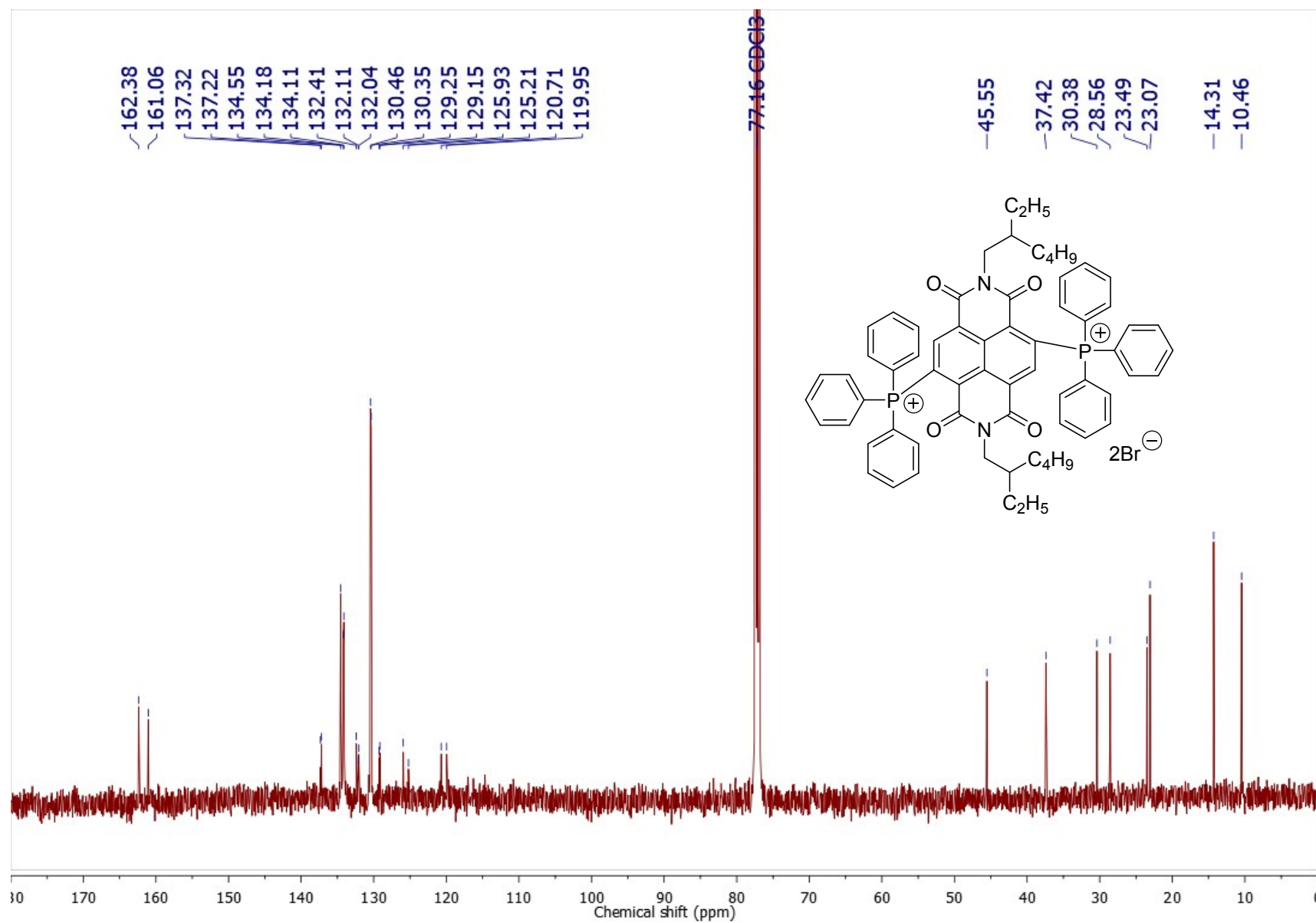


**Figure S16.**  $^{13}\text{C}$  NMR spectrum (500 MHz) of **1-2Br** in  $\text{CDCl}_3$ .

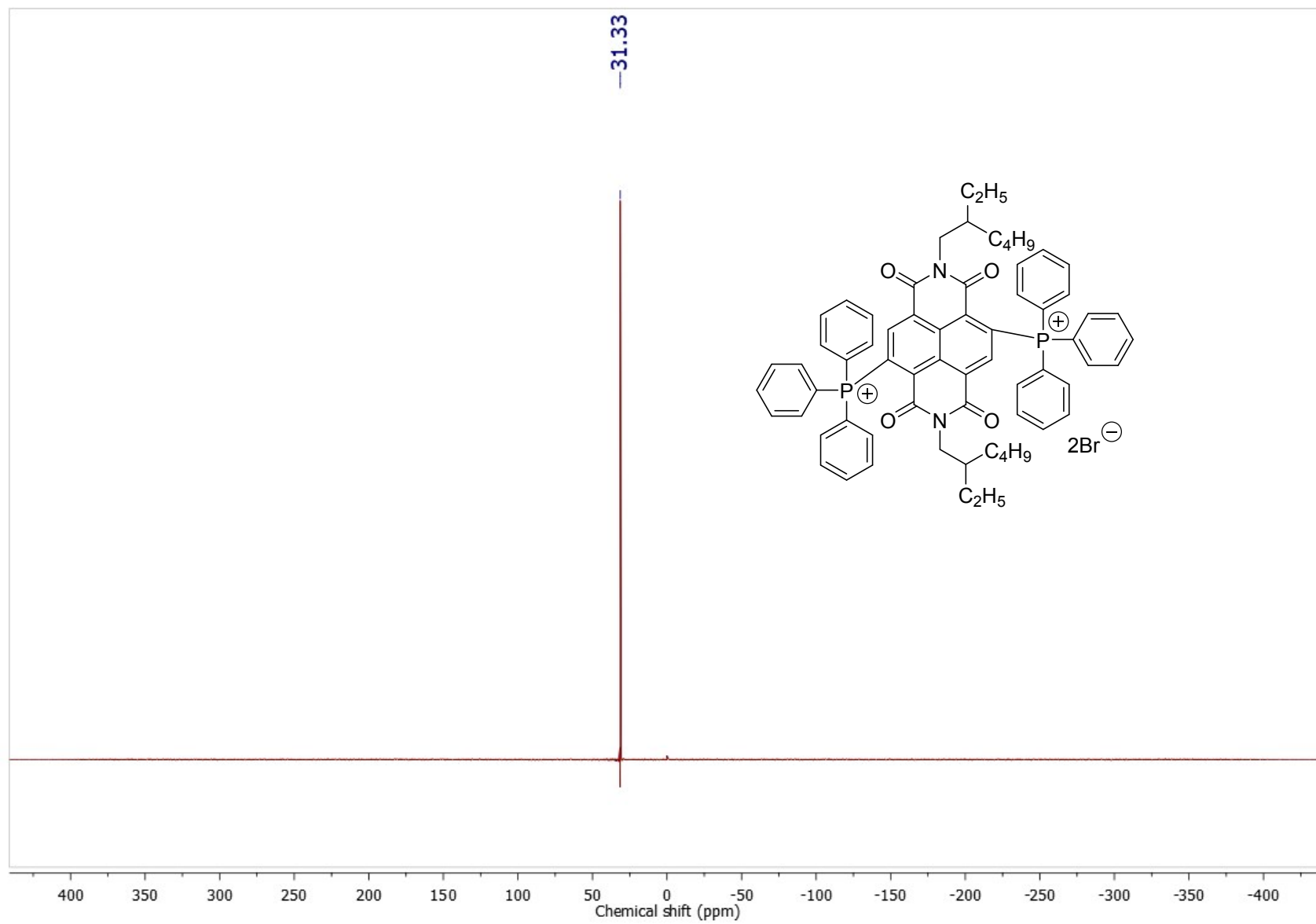


**Figure S17.**  $^{31}\text{P}$  NMR spectrum (500 MHz) of **1-2Br** in  $\text{CDCl}_3$ .

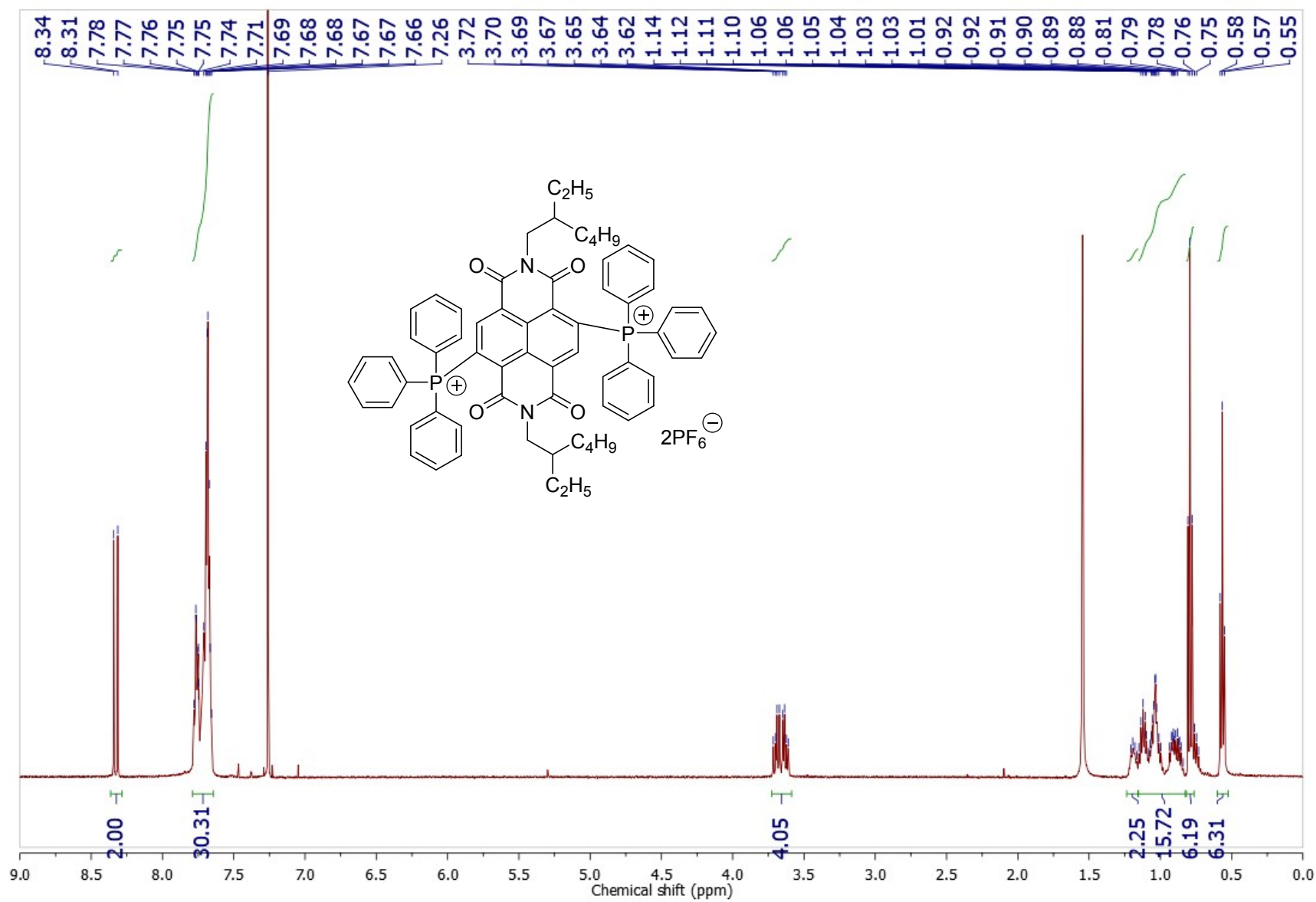
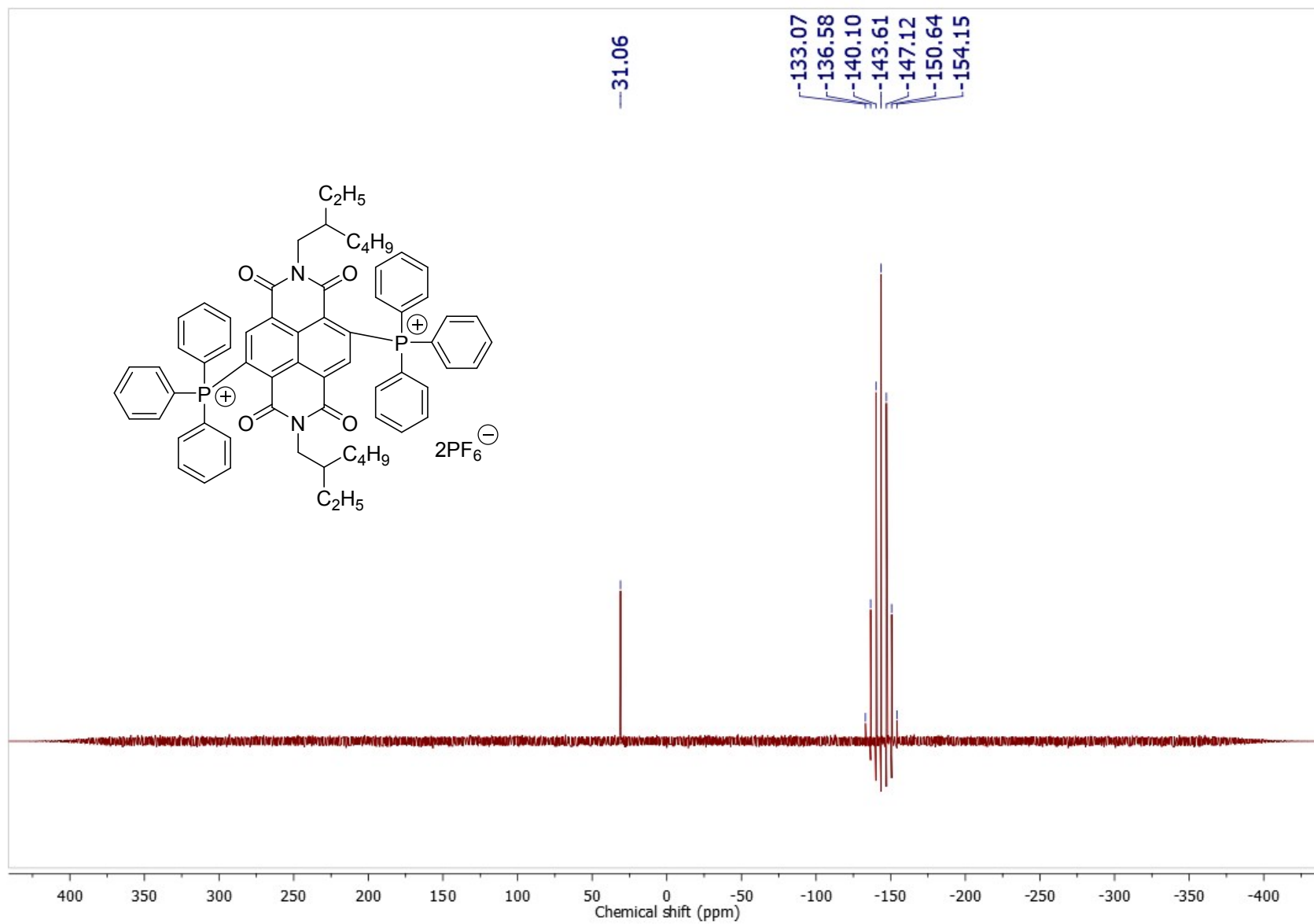
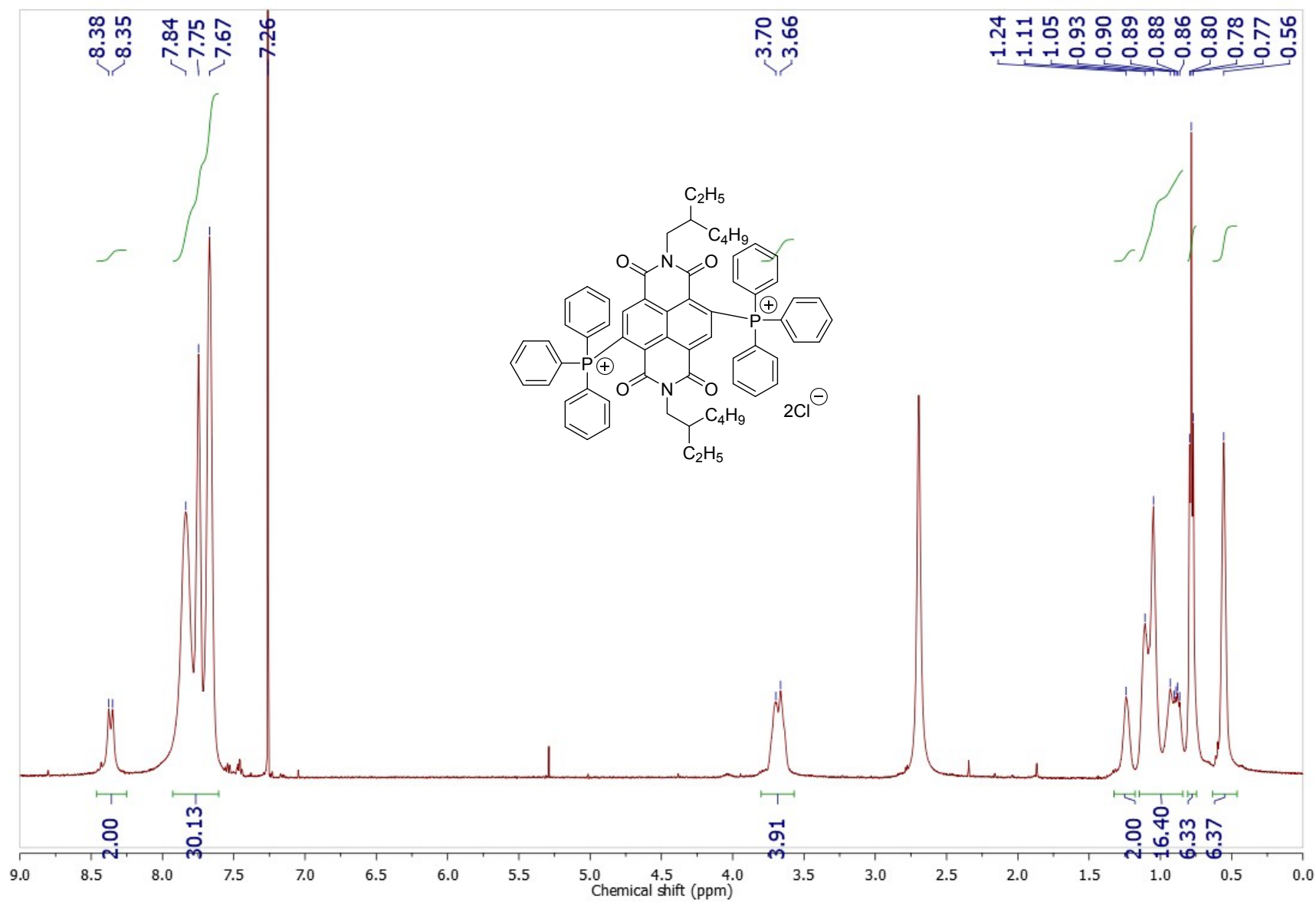


Figure S18.  $^1H$  NMR spectrum (500 MHz) of **1**- $2PF_6$  in  $CDCl_3$ .





**Figure S20.**  $^{31}\text{P}$  NMR spectrum (500 MHz) of **1-2PF<sub>6</sub>** in  $\text{CDCl}_3$ .



**Figure S21.** <sup>1</sup>H NMR spectrum (500 MHz) of **1-2Cl** in CDCl<sub>3</sub>.



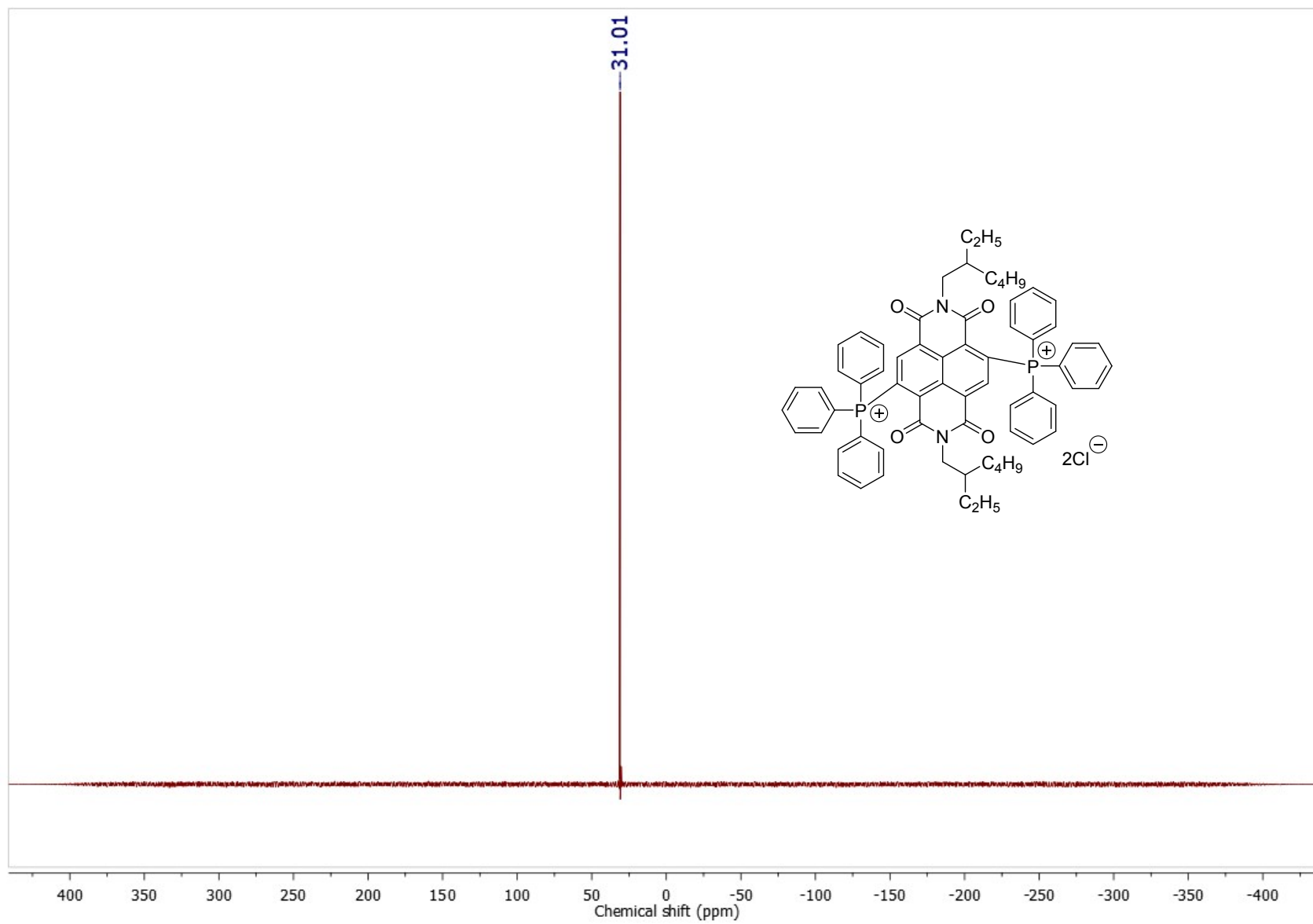


**Figure S23.**  $^{31}\text{P}$  NMR spectrum (500 MHz) of **1-2Cl** in  $\text{CDCl}_3$ .

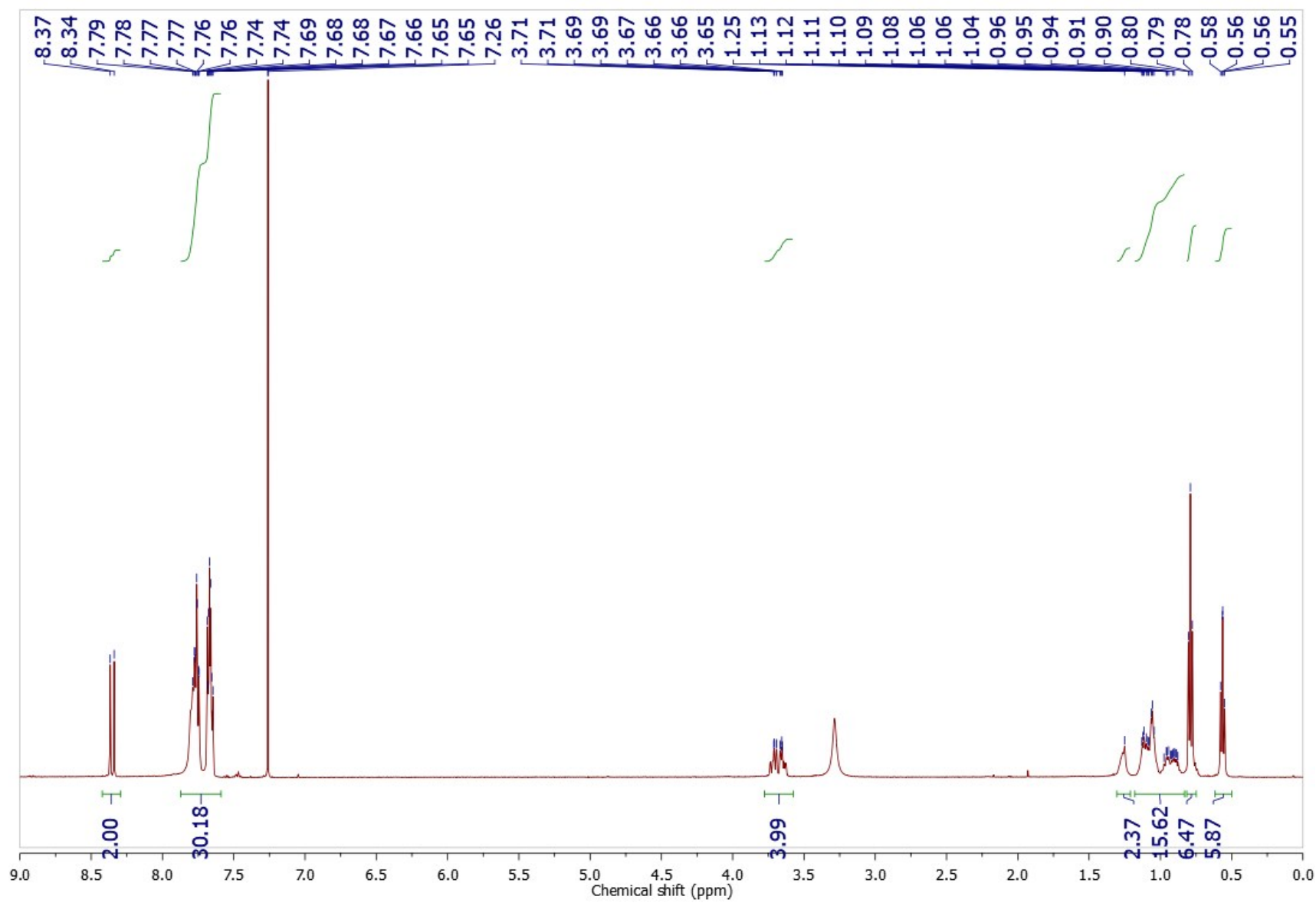


**Figure S24.**  $^1\text{H}$  NMR spectrum (500 MHz) of **1-2NO<sub>3</sub>** in  $\text{CDCl}_3$ .

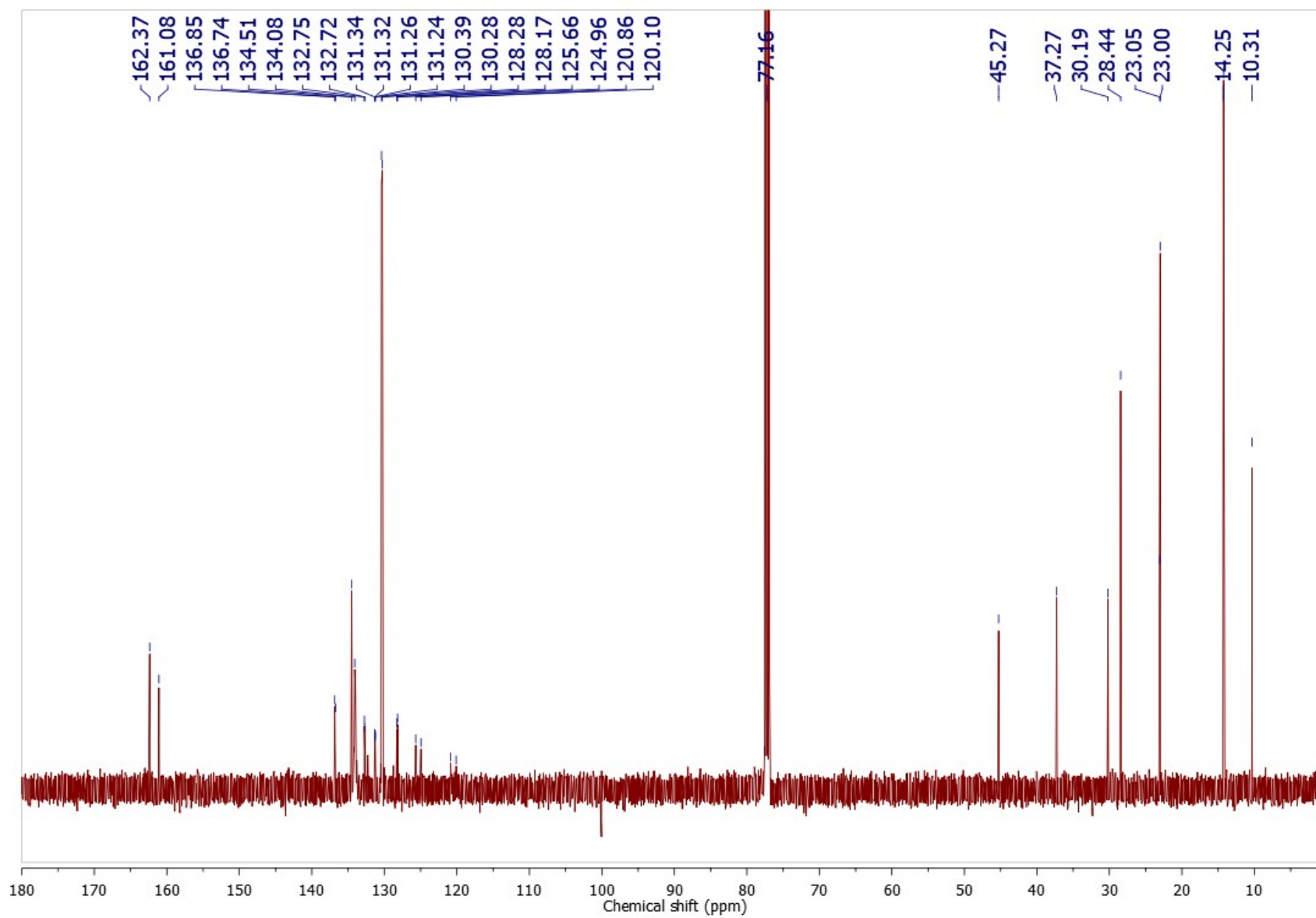
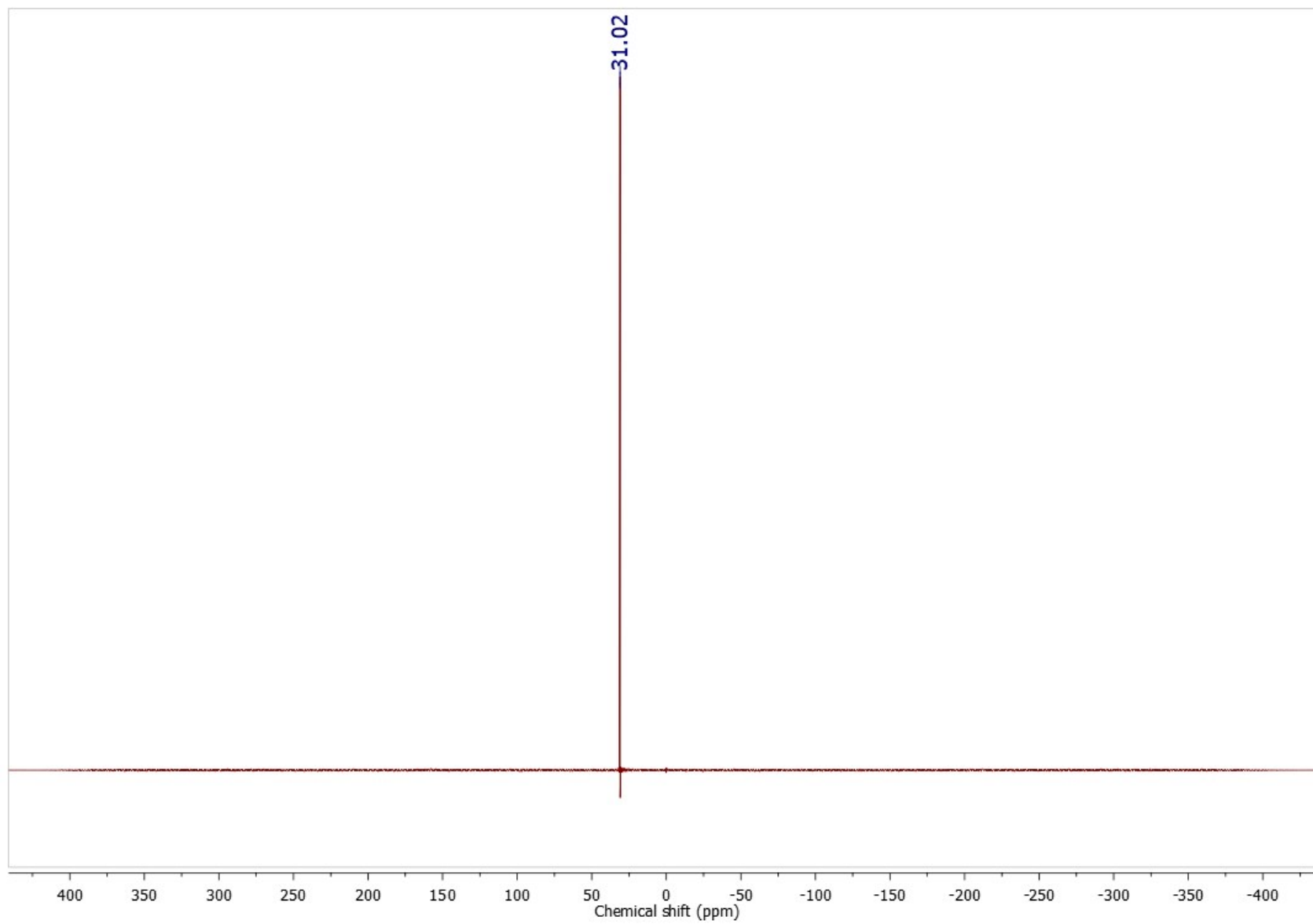
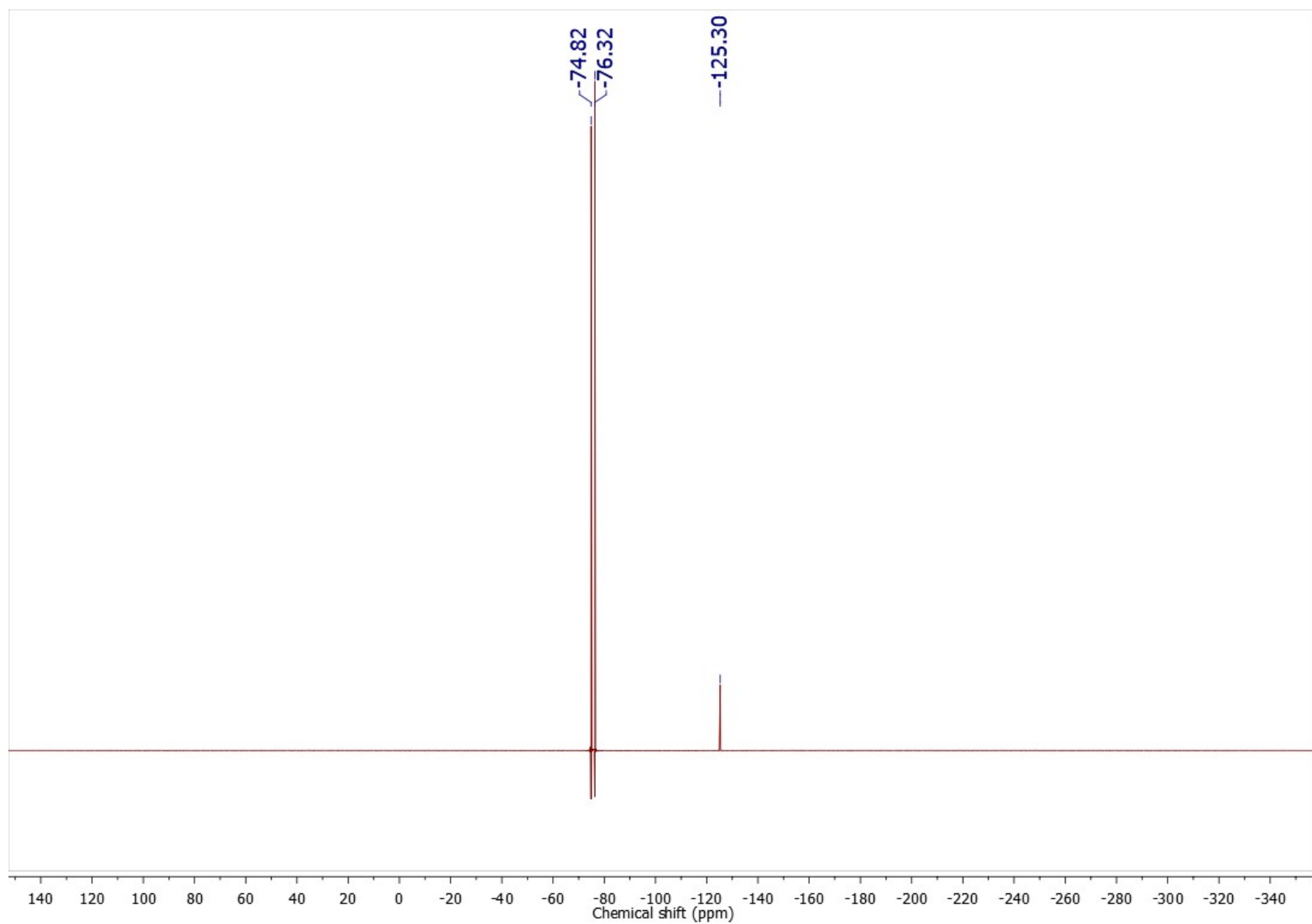


Figure S25.  $^{13}\text{C}$  NMR spectrum (500 MHz) of  $1\text{-}2\text{NO}_3$  in  $\text{CDCl}_3$ .



**Figure S26.**  $^{31}\text{P}$  NMR spectrum (500 MHz) of  $1\text{-}2\text{NO}_3$  in  $\text{CDCl}_3$ .



**Figure S27.**  $^{19}\text{F}$  NMR spectrum (470.39 MHz) of **TBA-PF<sub>6</sub>** in  $\text{CD}_3\text{CN}$ .

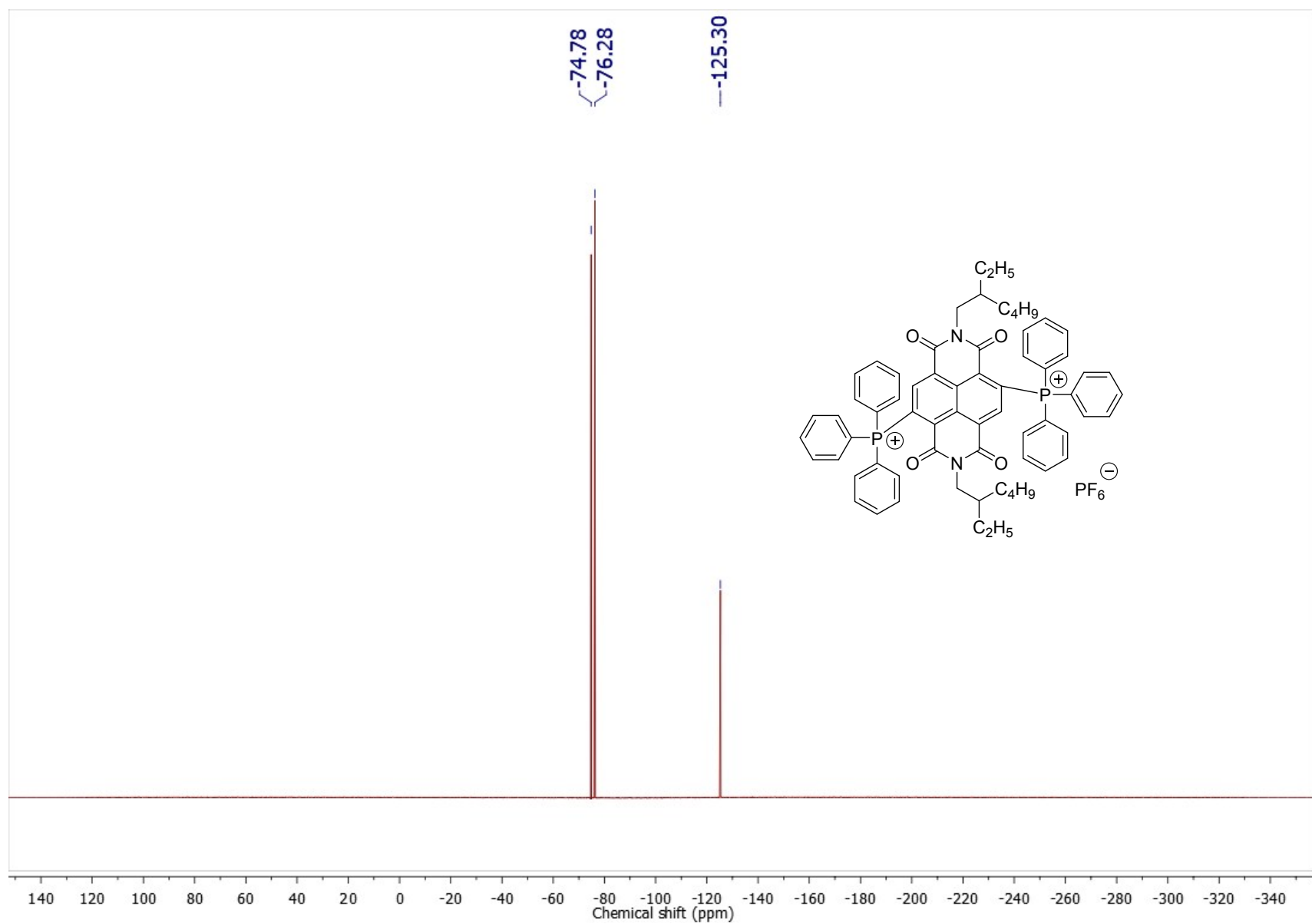


**Figure S28.**  $^{19}\text{F}$  NMR spectrum (470.39 MHz) of **1-PF<sub>6</sub>** in  $\text{CD}_3\text{CN}$ .

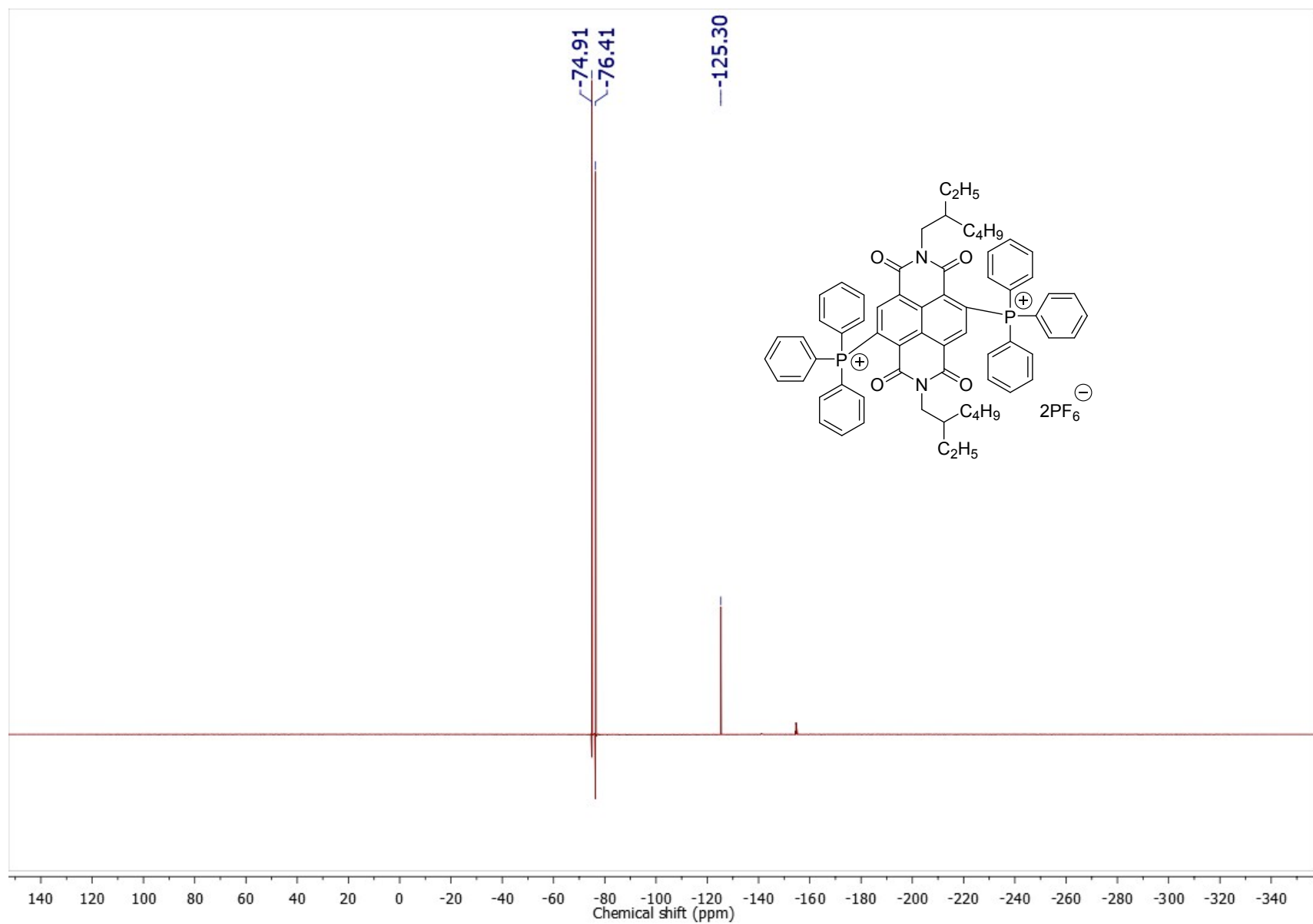


**Figure S29.**  $^{19}\text{F}$  NMR spectrum (470.39 MHz) of **1-2PF<sub>6</sub>** in  $\text{CD}_3\text{CN}$ .

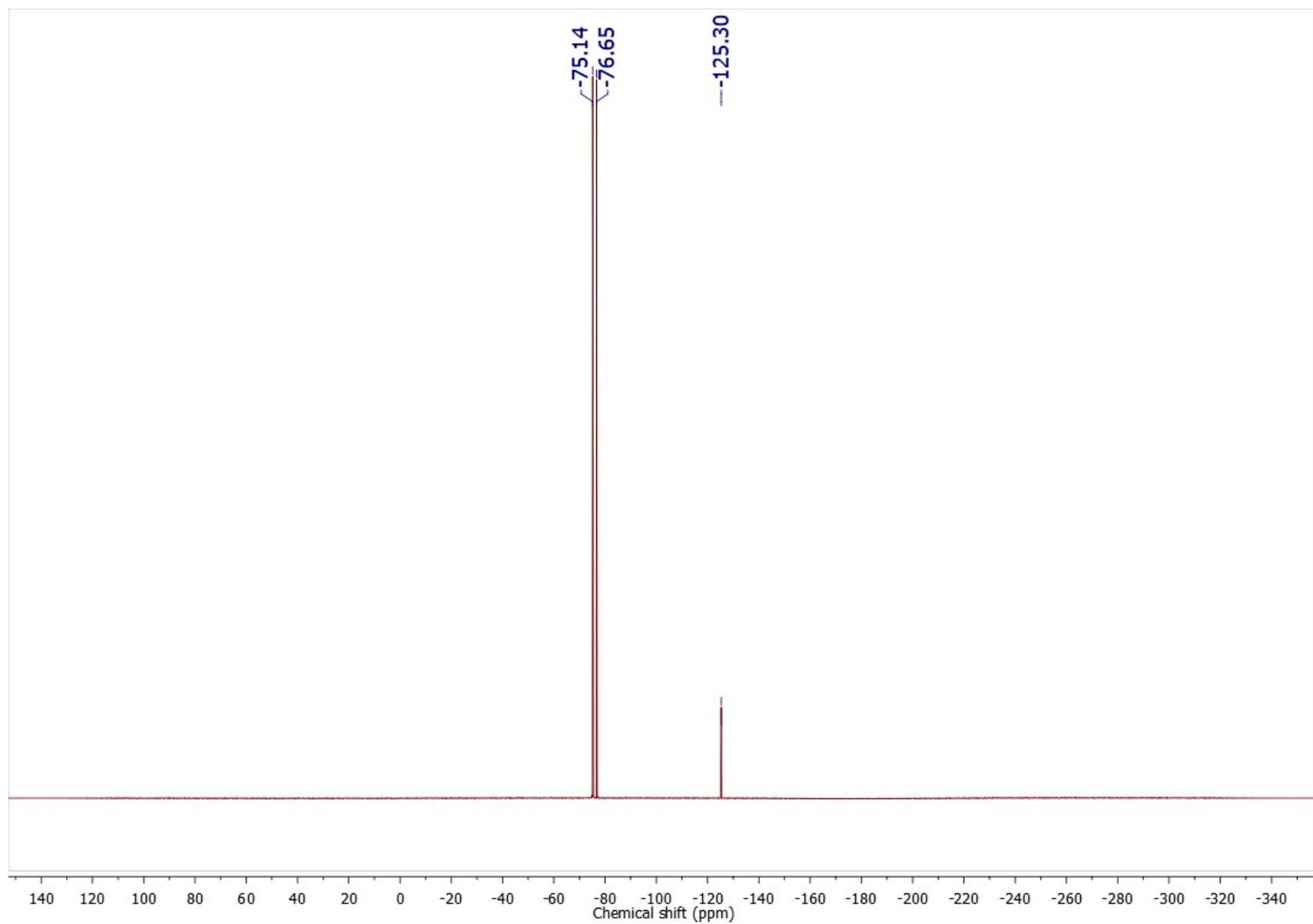


**Figure S30.**  $^{19}\text{F}$  NMR spectrum (470.39 MHz) of **TBA-PF<sub>6</sub>** in  $\text{CDCl}_3$ .

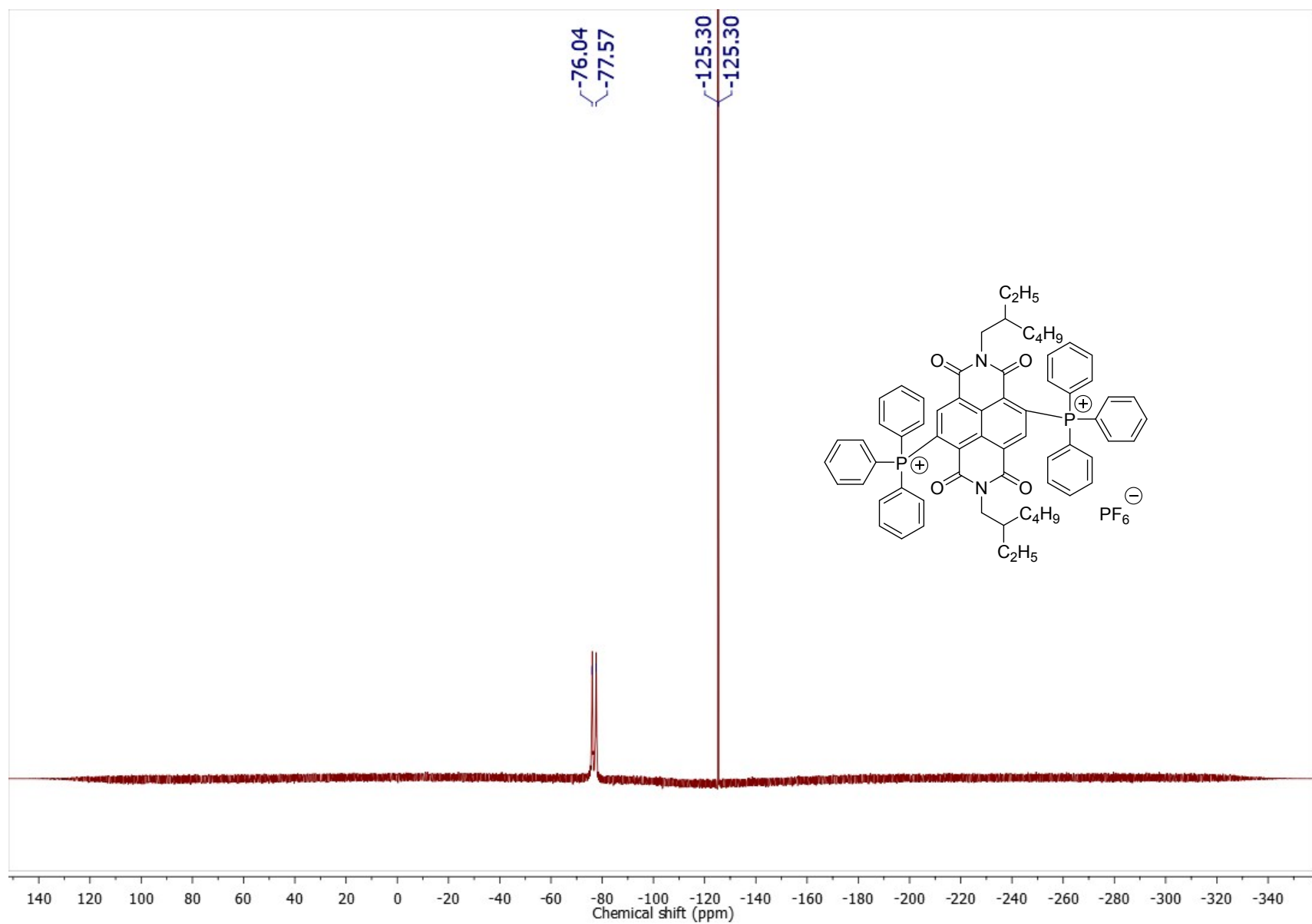


**Figure S31.**  $^{19}\text{F}$  NMR spectrum (470.39 MHz) of **1-PF<sub>6</sub>** in  $\text{CDCl}_3$ .

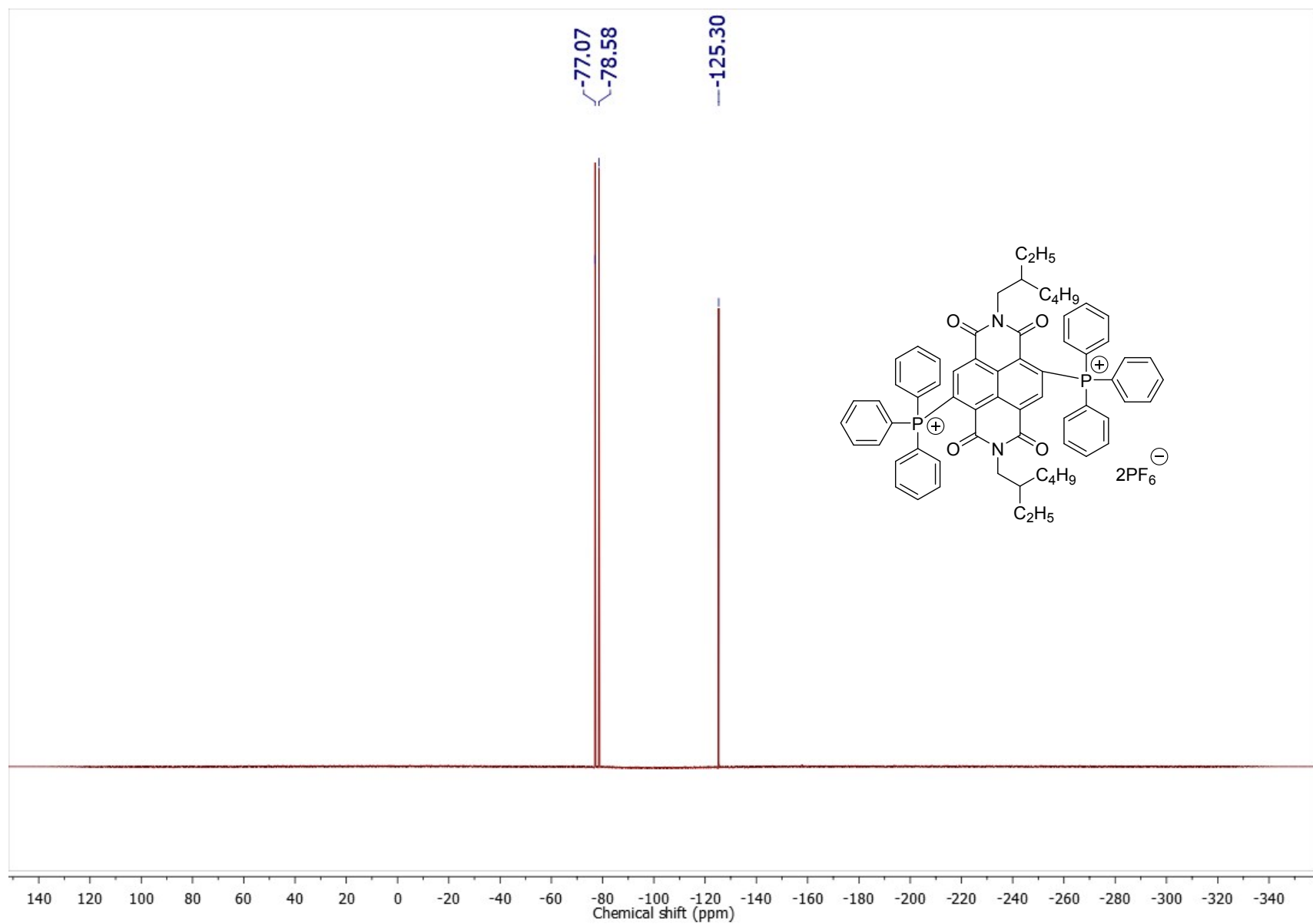


**Figure S32.**  $^{19}\text{F}$  NMR spectrum (470.39 MHz) of **1-2PF<sub>6</sub>** in  $\text{CDCl}_3$

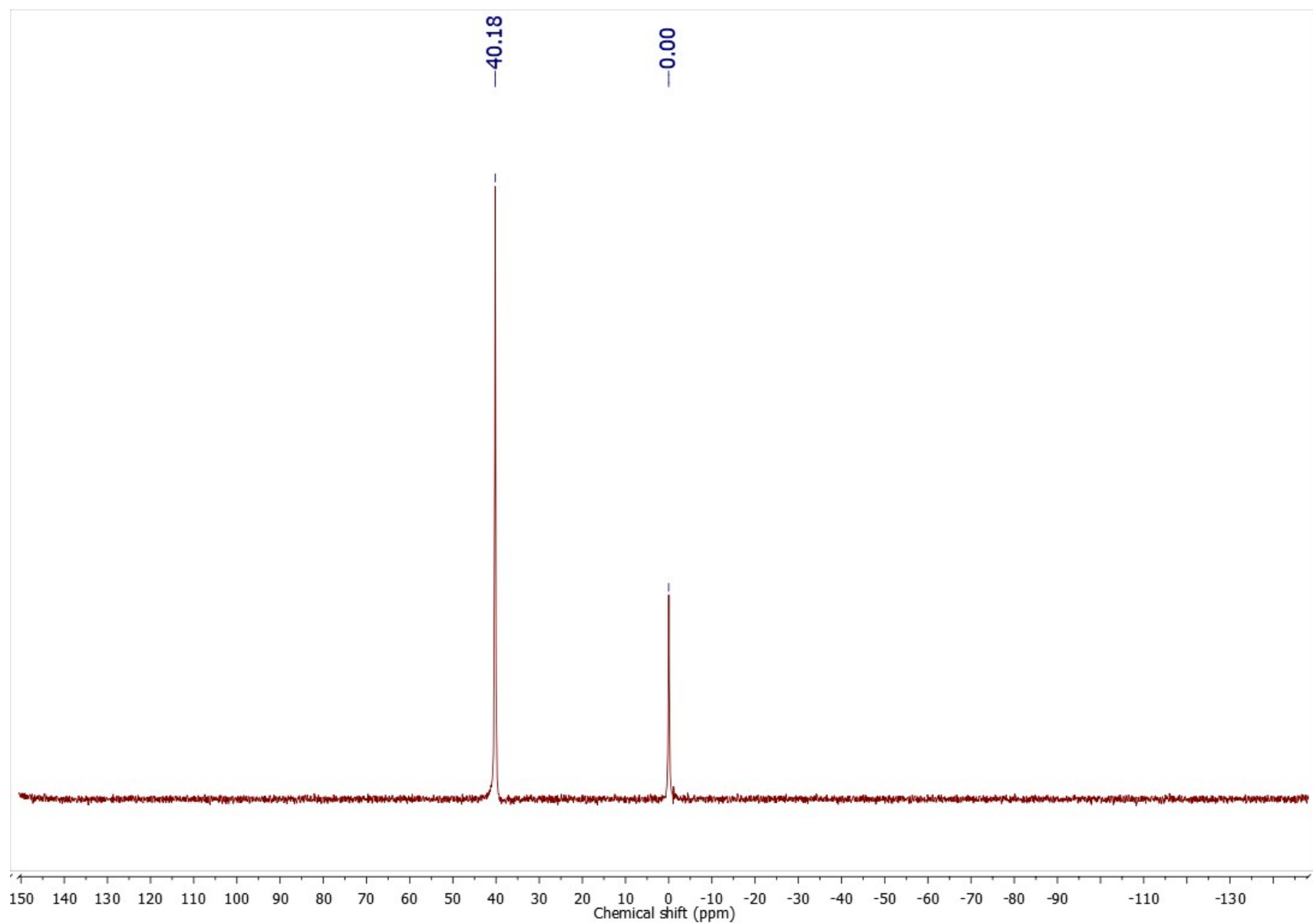


**Figure S33.**  $^{35}\text{Cl}$  NMR spectrum (49.94 MHz) of **TBA-Cl** in  $\text{CD}_3\text{CN}$ .

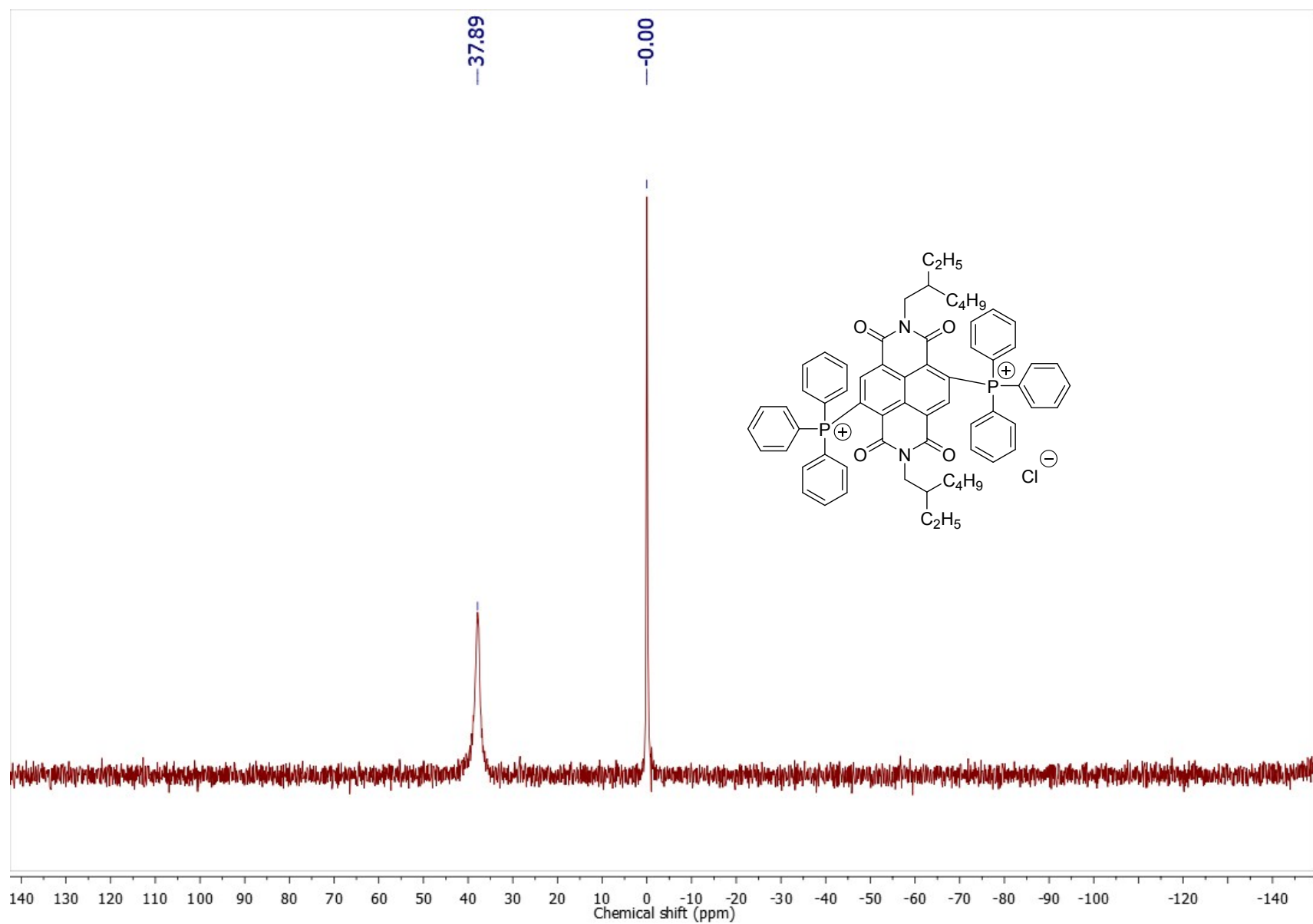


**Figure S34.**  $^{35}\text{Cl}$  NMR spectrum (49.94 MHz) of **1-Cl** in  $\text{CD}_3\text{CN}$ .

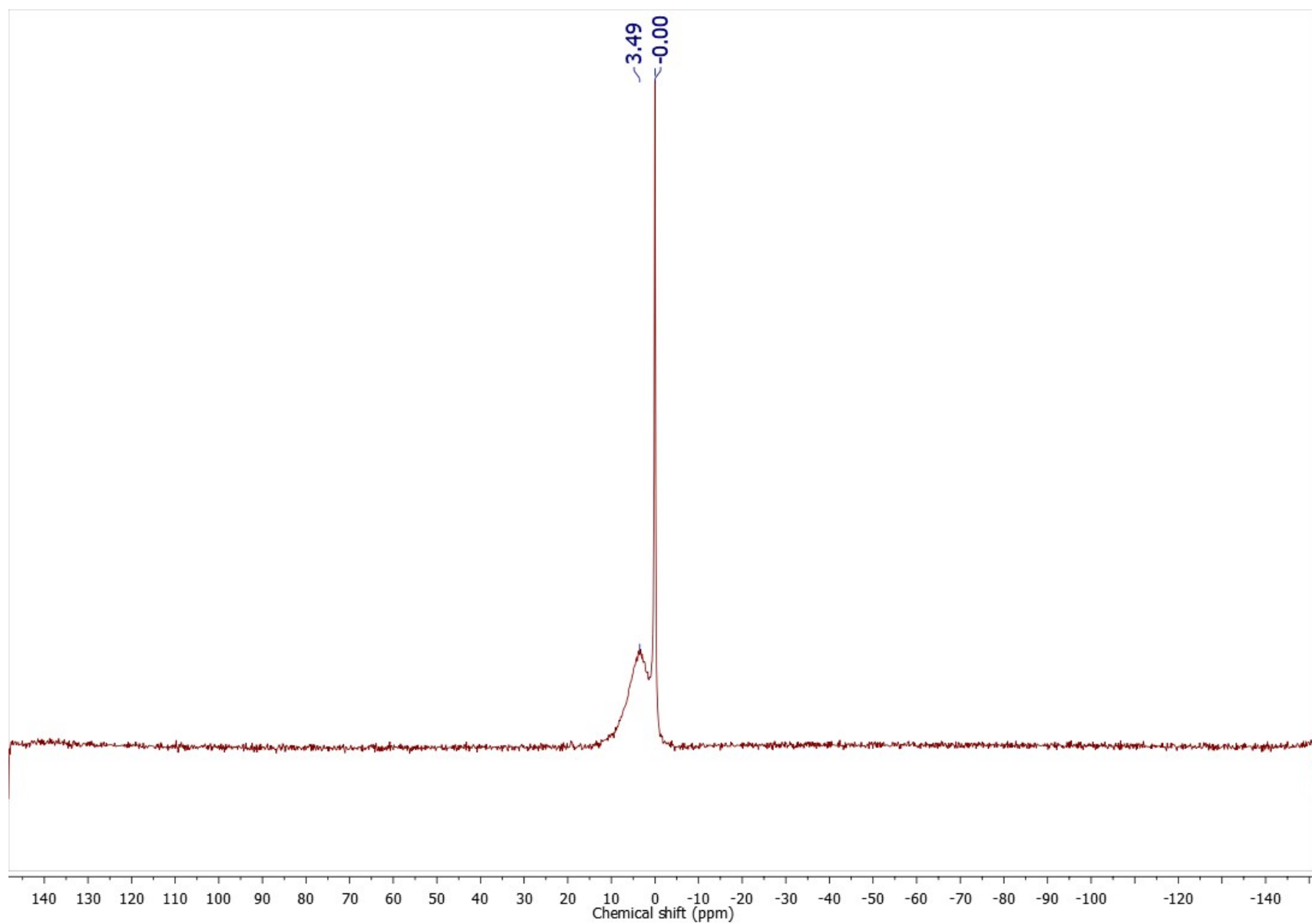


**Figure S35.**  $^{35}\text{Cl}$  NMR spectrum (49.94 MHz) of **TBA-Cl** in  $\text{CDCl}_3$ .

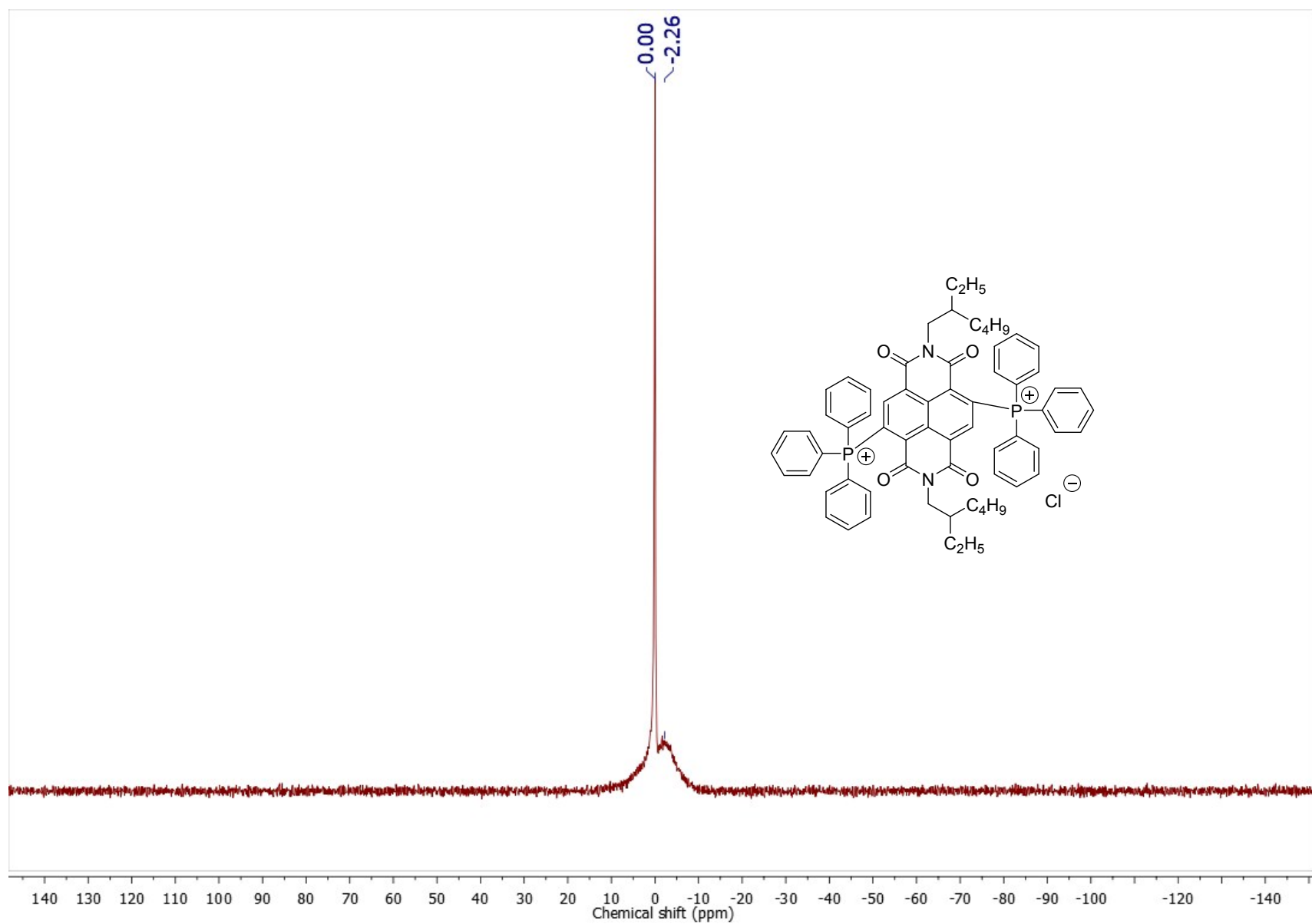


**Figure S36.**  $^{35}\text{Cl}$  NMR spectrum (49.94 MHz) of **1-Cl** in  $\text{CDCl}_3$ .

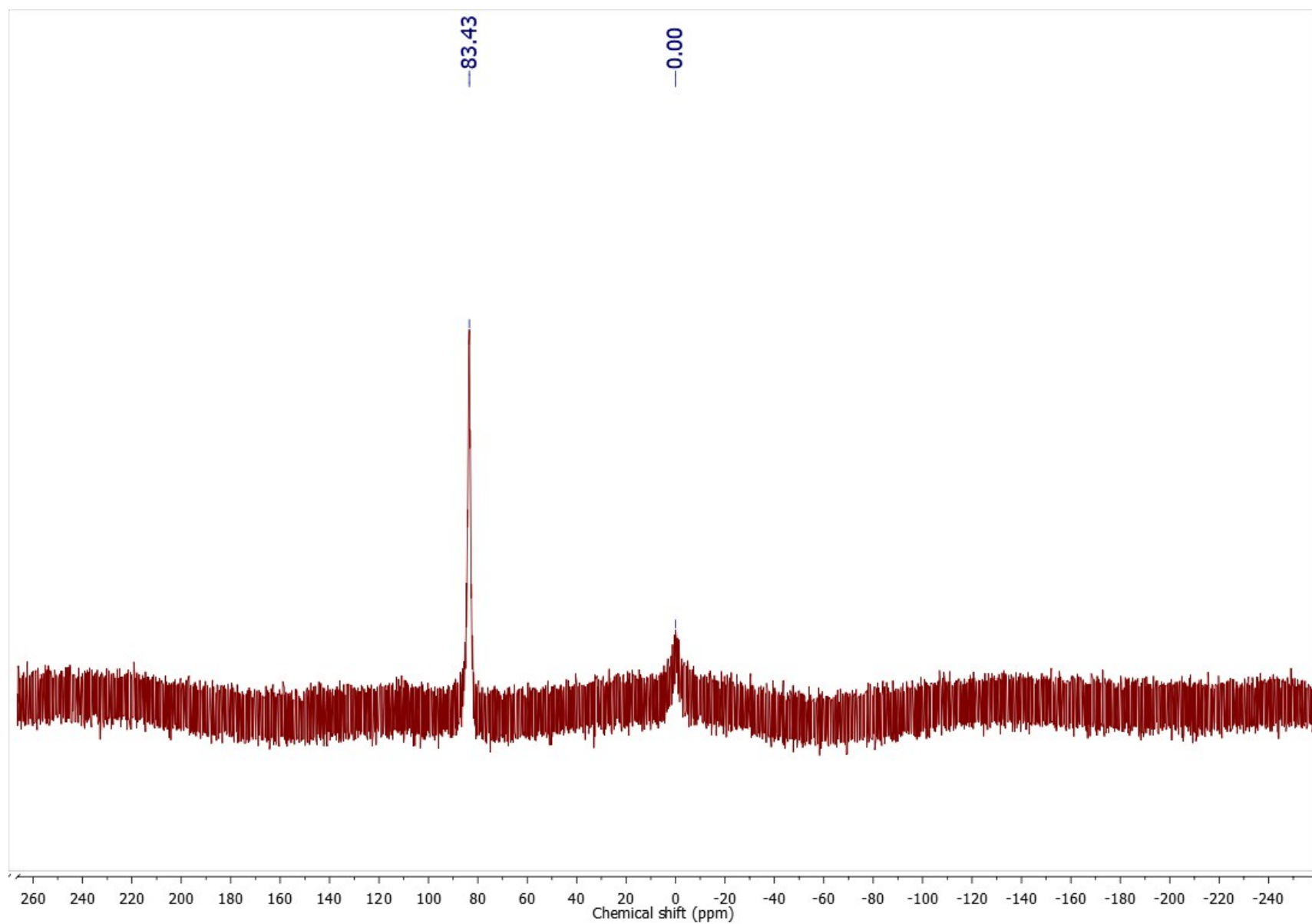


**Figure S37.**  $^{81}\text{Br}$  NMR spectrum (134.89 MHz) of **TBA-Br** in  $\text{CD}_3\text{CN}$ .

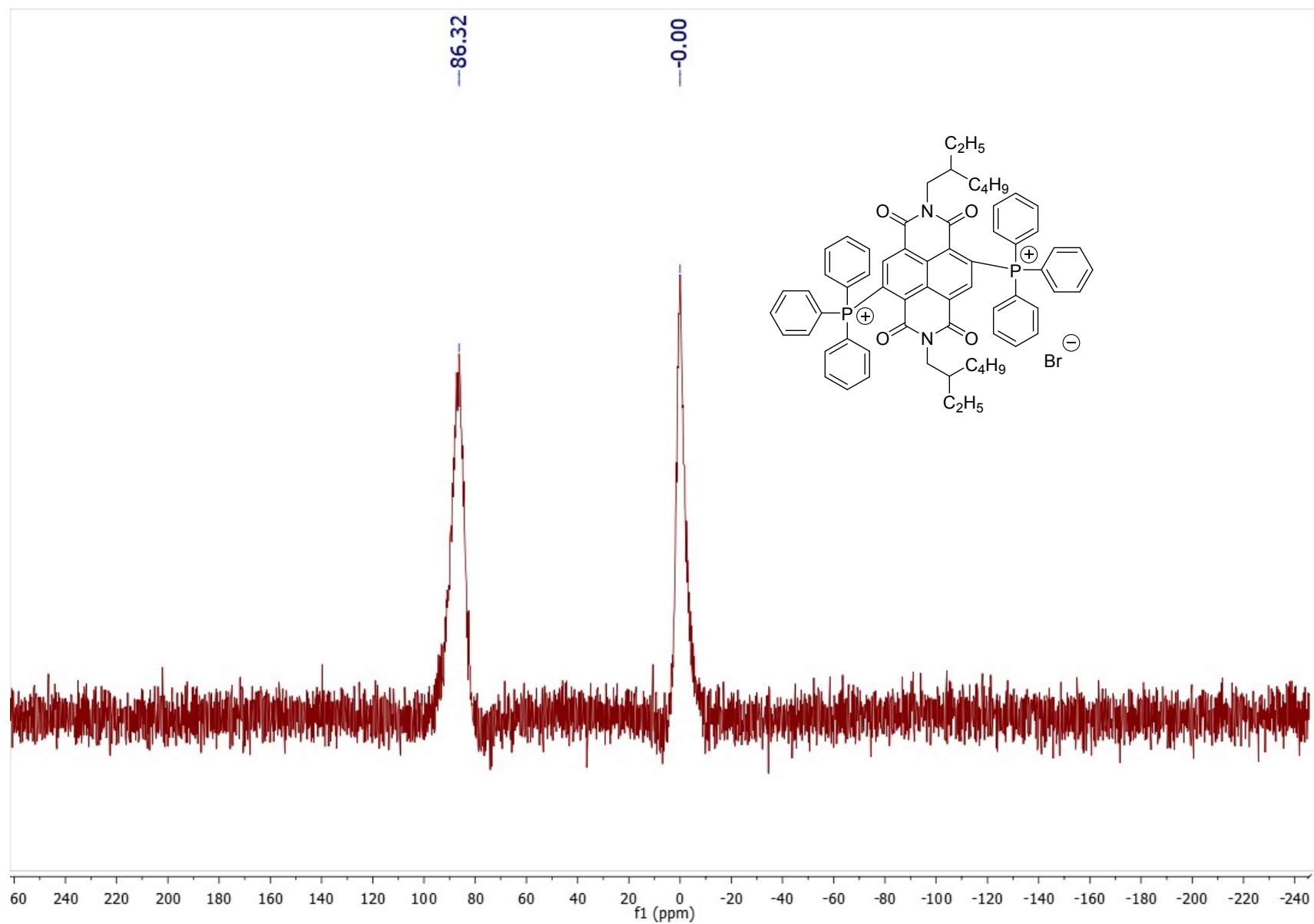


**Figure S38.**  $^{81}\text{Br}$  NMR spectrum (134.89 MHz) of **1-Br** in  $\text{CD}_3\text{CN}$ .

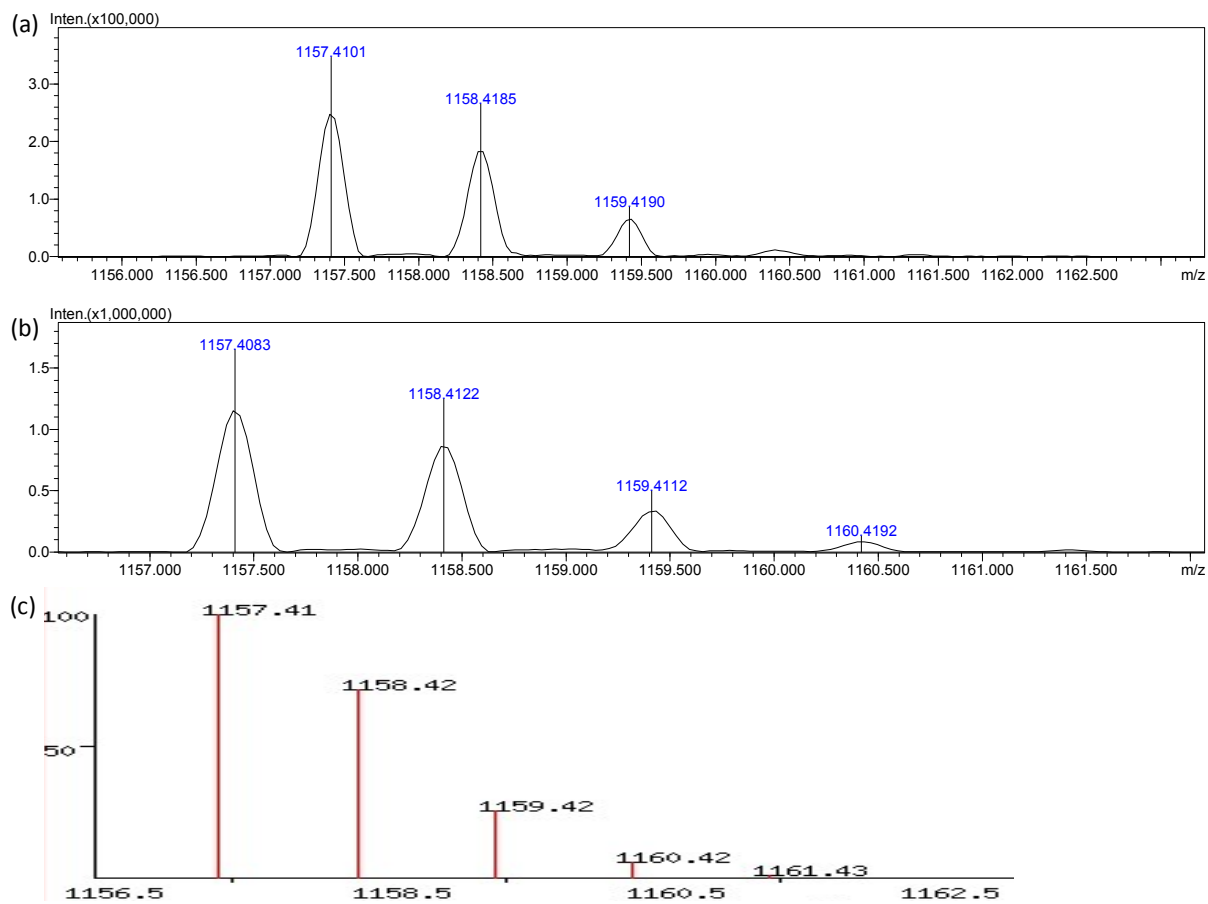


**Figure S39.** (a) ESI-MS (positive mode) experimental isotopic distribution pattern of 1-PF<sub>6</sub>. (b) ESI-MS (positive mode) experimental isotopic distribution pattern of 1-2PF<sub>6</sub>. (c) Predicted isotopic distribution for [1+PF<sub>6</sub>]<sup>+</sup>.

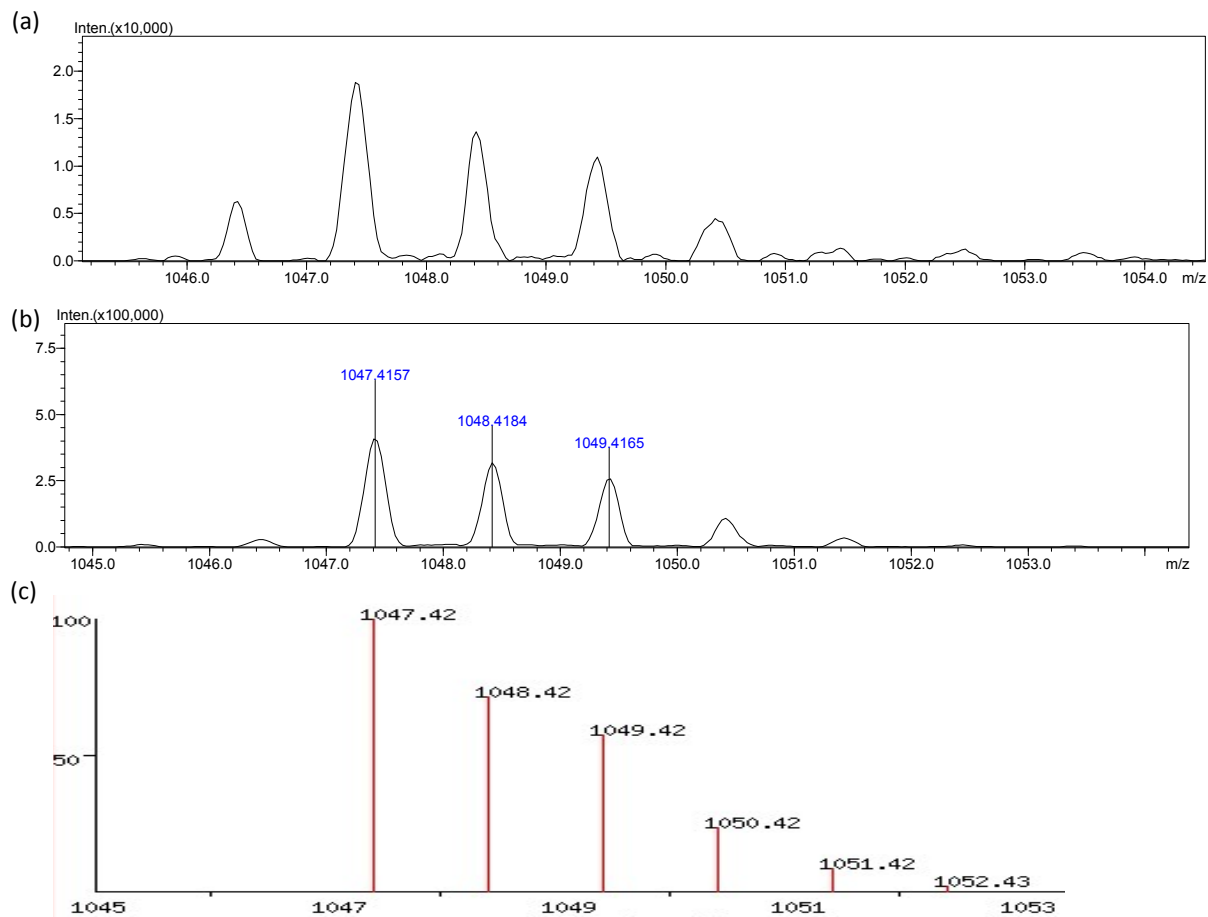


**Figure S40.** (a) ESI-MS (positive mode) experimental isotopic distribution pattern of 1-Cl. (b) ESI-MS (positive mode) experimental isotopic distribution pattern of 1-2Cl. (c) Predicted isotopic distribution for  $[1+Cl]^+$ .

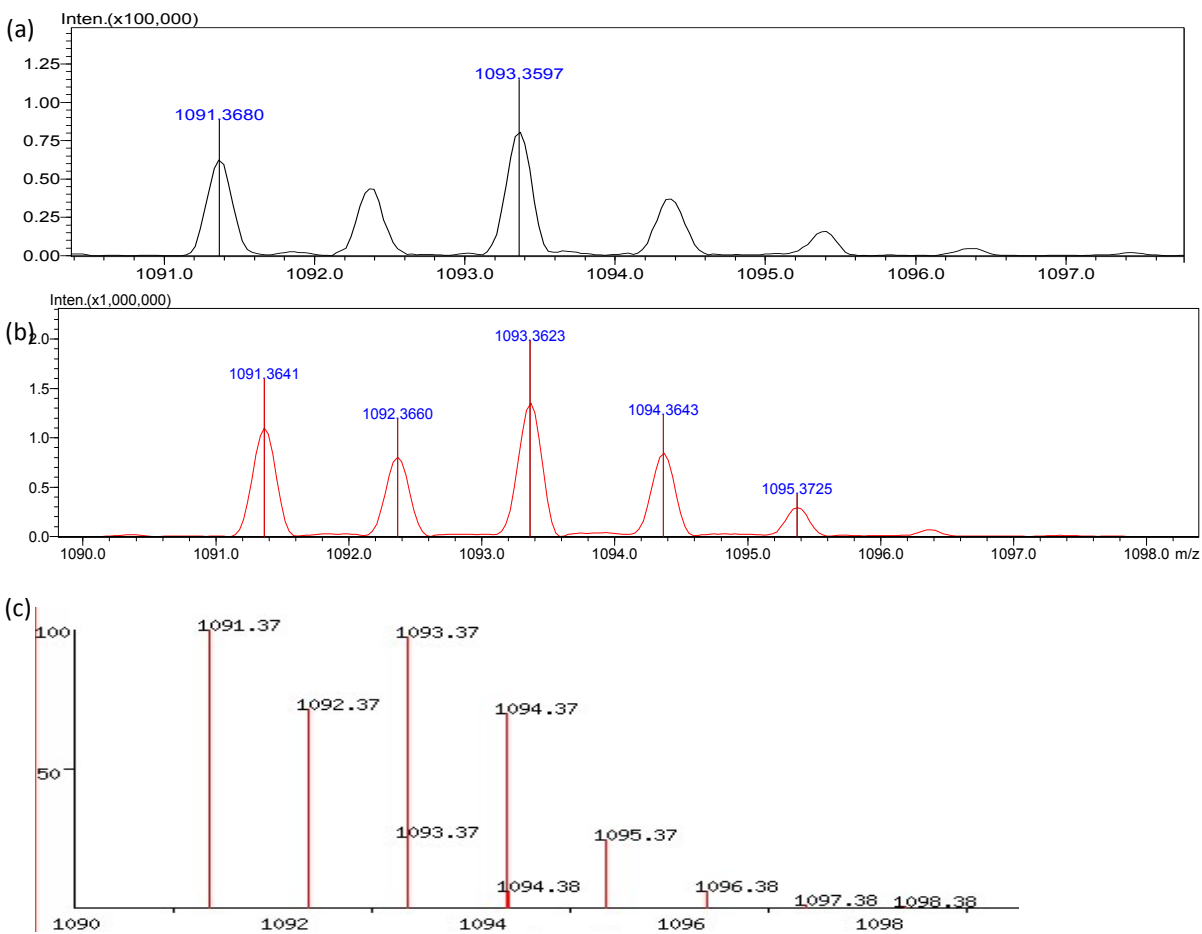


**Figure S41.** (a) ESI-MS (positive mode) experimental isotopic distribution pattern of 1-Br. (b) ESI-MS (positive mode) experimental isotopic distribution pattern of 1-2Br. (c) Predicted isotopic distribution for  $[1+\text{Br}]^+$ .

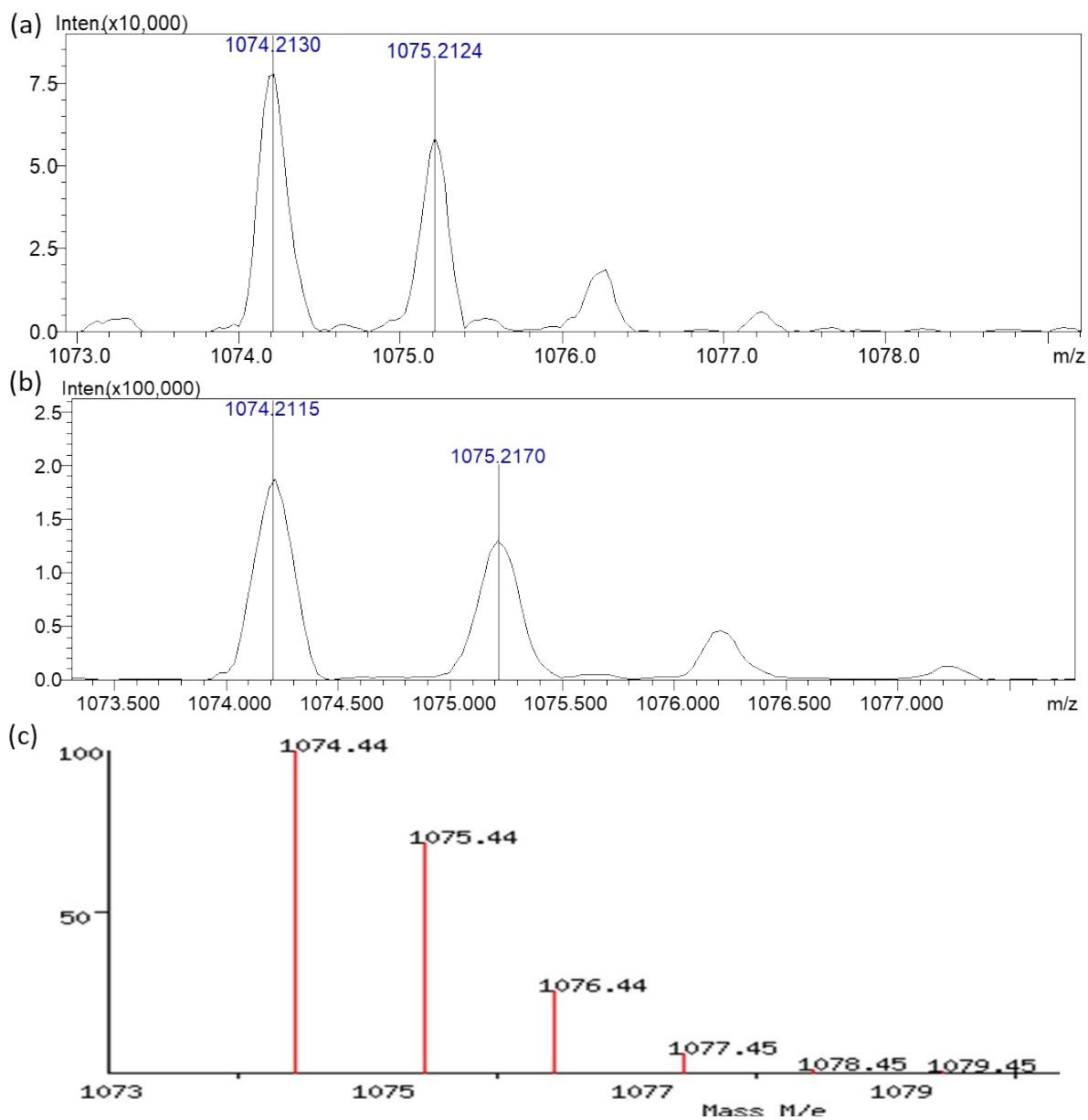


**Figure S42.** (a) ESI-MS (positive mode) experimental isotopic distribution pattern of 1-NO<sub>3</sub>. (b) ESI-MS (positive mode) of experimental isotopic distribution pattern of 1-2 NO<sub>3</sub>. (c) Predicted isotopic distribution for [1+ NO<sub>3</sub>]<sup>+</sup>.

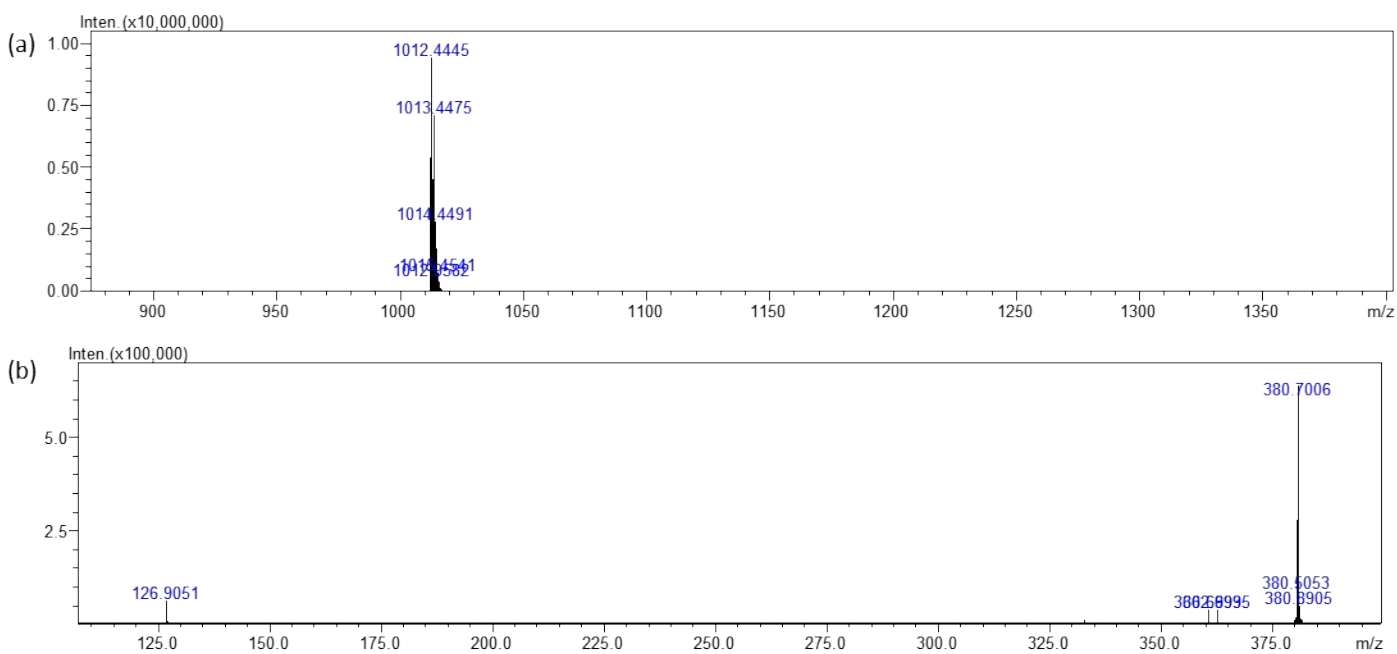


**Figure S43.** (a) ESI-MS (positive mode) of experimental isotopic distribution pattern of **1-I** which shows  $[1]^+$  at 1012.44. (b) ESI-MS (negative) of experimental isotopic distribution pattern of **1-I** which shows mostly  $I_3^-$  at 380.70 with a small amount of  $I^-$  at 126.91.

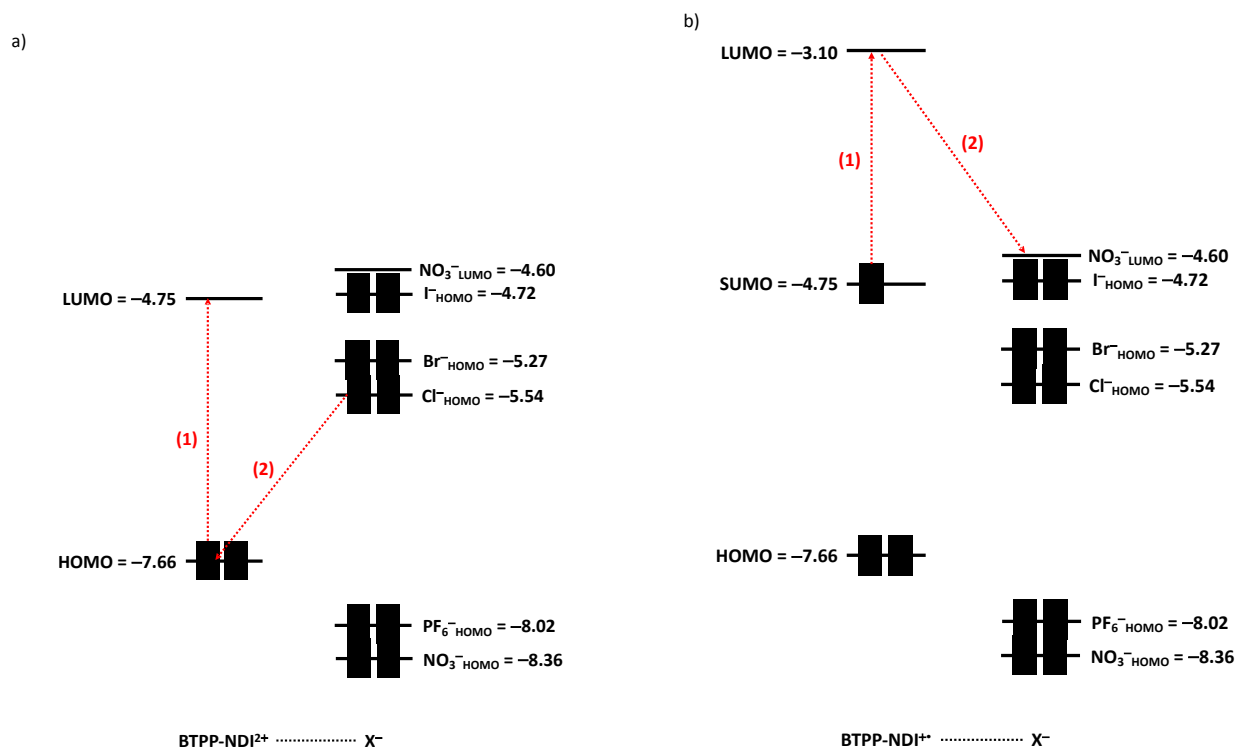


**Figure S44.** a) “Normal” PET for **1-2Cl**. (1) Photoexcitation of the BTTP-NDI<sup>2+</sup> resulted in HOMO→LUMO transition, followed by (2) electron transfer from the Cl<sup>-</sup> to the photoexcited BTTP-NDI<sup>2+</sup>. This electron transfer occurs in both acetonitrile and chloroform, and is only possible in the more Lewis basic Cl<sup>-</sup> rather than Br<sup>-</sup> (PF<sub>6</sub><sup>-</sup> and NO<sub>3</sub><sup>-</sup> do not have accessible HOMO), indicating Lewis basicity is important for “normal” PET to occur. The HOMO value of I<sup>-</sup> is slightly higher than the LUMO value of BTTP-NDI<sup>2+</sup>. Thermal electron transfer occurs readily and this explains why the 2+ iodide cannot be isolated. b) “Reverse” PET for **1-NO<sub>3</sub>**. (1) Photoexcitation of the BTTP-NDI<sup>+•</sup> resulted in SUMO→LUMO transition as predicted by TDDFT, followed by (2) electron transfer from the LUMO of the photoexcited BTTP-NDI<sup>+•</sup> to the LUMO of NO<sub>3</sub><sup>-</sup>. This electron transfer occurs only in chloroform and not in acetonitrile, indicating *pK<sub>a</sub>* of the solvent (acetonitrile = 25, chloroform = 15.5) is also important for this PET to occur. This is due to the fact that reduction of NO<sub>3</sub><sup>-</sup> requires the presence of H<sup>+</sup> as stated in the redox equation: NO<sub>3</sub><sup>-</sup> + 2H<sup>+</sup> + 2e<sup>-</sup> → NO<sub>2</sub><sup>-</sup> + 2H<sub>2</sub>O. HOMO value of BTTP-NDI<sup>2+</sup> is estimated from its LUMO value (from CV measurement) and optical bandgap of **1-2PF<sub>6</sub>** (426 nm, 2.91 eV). LUMO value of BTTP-NDI<sup>+•</sup> is estimated from its SUMO value (from CV measurement) and optical bandgap of the 1+ salts (750 nm, 1.65eV). HOMO value of NO<sub>3</sub><sup>-</sup> is

estimated from its LUMO value ( $\text{NO}_3^- + 2\text{H}^+ + 2\text{e}^- \rightarrow \text{NO}_2^- + 2\text{H}_2\text{O}$ ,  $E^\circ = +0.42 \text{ V}$ ;<sup>3</sup>  $\text{Fc}/\text{Fc}^+$  vs SHE = +0.62 V;<sup>4</sup> HOMO of Fc = 4.8 eV) and optical bandgap (330 nm, 3.76 eV).<sup>5</sup> HOMO values of  $\text{PF}_6^-$ ,  $\text{Cl}^-$ ,  $\text{Br}^-$  and  $\text{I}^-$  have been previously derived.<sup>6</sup>

## 5. References

1. R. Belcher, J. E. Fildes and A. J. Nutten, *Anal. Chim. Acta*, 1955, **13**, 431-436.
2. S. Kumar, M. R. Ajayakumar, G. Hundal and P. Mukhopadhyay, *J. Am. Chem. Soc.*, 2014, **136**, 12004-12010.
3. B. C. Berks, S. J. Ferguson, J. W. B. Moir and D. J. Richardson, *Biochimica et Biophysica Acta (BBA) - Bioenergetics*, 1995, **1232**, 97-173.
4. V. V. Pavlishchuk and A. W. Addison, *Inorg. Chim. Acta*, 2000, **298**, 97-102.
5. J. Mack and J. R. Bolton, *Journal of Photochemistry and Photobiology A: Chemistry*, 1999, **128**, 1-13.
6. T. L. D. Tam, C. K. Ng, X. Lu, Z. L. Lim and J. Wu, *Chem. Commun.*, 2018, **54**, 7374-7377.